

RKKY interaction in triplet superconductors: Dzyaloshinskii–Moriya-type interaction mediated by spin-polarized Cooper pairs

Jabir Ali Ouassou and Jacob Linder

Center for Quantum Spintronics, Department of Physics, Norwegian
University of Science and Technology, NO-7491 Trondheim, Norway

Takehito Yokoyama

Department of Physics, Tokyo Institute of Technology, Meguro, Tokyo 152-8551, Japan

The Ruderman–Kittel–Kasuya–Yosida (RKKY) interaction governs the coupling between localized spins and is strongly affected by the environment in which these spins reside. In superconductors, this interaction becomes long-ranged and provides information about the orbital symmetry of the superconducting order parameter. In this work, we consider the RKKY interaction between localized spins mediated by a p -wave triplet superconductor. In contrast to the well-studied RKKY interaction in d -wave superconductors, we find that the spin of the Cooper pair in a triplet state also modulates the spin–spin coupling. We consider several different types of p -wave triplet states, and find that the form of the RKKY interaction changes significantly with the symmetries of the order parameter. For non-unitary superconducting states, two new terms appear in the RKKY interaction: a background spin magnetization coupling to the individual spins and, more interestingly, an effective Dzyaloshinskii–Moriya term. The latter term oscillates with the separation distance between the impurity spins. Finally, we find that the finite spin expectation value in non-unitary superconductors in concert with the conventional RKKY interaction can lead to non-collinear magnetic ground states even when the Dzyaloshinskii–Moriya term is negligible. The RKKY interaction in p -wave triplet superconductors thus offers a way to achieve new ground state spin configurations of impurity spins and simultaneously provides information about the underlying superconducting state.

I. INTRODUCTION

Two localized spins can interact via itinerant spin carriers in a material. In metals, this interaction is usually mediated by electrons. This effect is known as a Ruderman–Kittel–Kasuya–Yosida (RKKY) interaction [1–3] or an indirect exchange interaction. The mechanism can be understood as follows. When itinerant electrons approach a localized spin, the wave functions of spin-up and spin-down electrons are scattered in different ways. This creates “ripples” in the net spin density, whereby the spin expectation value of the itinerant electrons oscillates and decays as a function of the distance from the localized spin. When a second localized spin then couples to the itinerant electrons, its lowest-energy spin orientation depends on whether it has been placed in a peak or trough of the spin density generated by the first localized spin. The net interaction between the spins can thus be either ferromagnetic or antiferromagnetic, depending on their separation distance.

The RKKY interaction is interesting for several reasons. One is the possibility to tune the interaction, and thus the preferred alignment, of two localized spins via the system in which they are embedded. Conversely, the behavior of the spin–spin interaction can provide important information about other interactions in the system. Thus, the RKKY interaction has been subject of thorough investigation in a number of different classes of systems: low-dimensional electron gases [4, 5], normal metals [1–3], superconductors [6–10], and topological insulators [11–13], to mention some examples.

When two localized spins are placed on the surface of a superconductor (see Fig. 1), their RKKY interaction can provide important information about the superconducting order parameter. A conventional BCS superconductor [14] has s -wave singlet symmetry, i.e. electrons experience an isotropic order

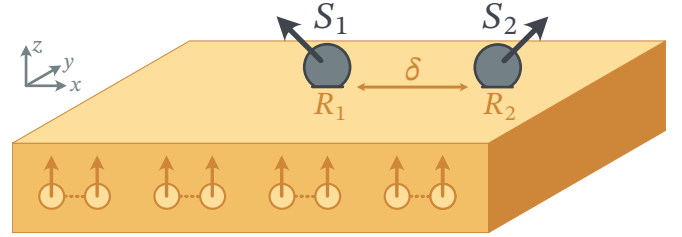


FIG. 1. We consider a 2D superconductor in the xy plane, which hosts a condensate of p -wave spin-triplet Cooper pairs. Two classical spins S_1 and S_2 are placed on top of this superconductor; S_1 at the center, S_2 displaced along the x axis by $\delta = |\mathbf{R}_2 - \mathbf{R}_1|$. Herein, we investigate how the RKKY interaction between S_1 and S_2 is affected by unconventional superconductivity. Numerically, we consider a square lattice of dimensions $280a \times 40a$ with open boundary conditions, such that $\mathbf{R}_1 = (140a, 20a)$ and $\mathbf{R}_2 = (140a + \delta, 20a)$. Analytically, we consider an infinite translation-invariant superconductor, where only the displacement $\mathbf{R}_2 - \mathbf{R}_1$ is relevant. Both the numerics and analytics show that the RKKY interaction is sensitive to the spin and momentum symmetries of the order parameter, and can thus potentially be used to classify unconventional superconductors.

parameter $\Delta(\mathbf{p}) = \Delta_0$ that is independent of the direction of momentum \mathbf{p} of the electrons. In contrast, a high- T_c superconductor with d -wave singlet symmetry features an anisotropic gap in momentum space, e.g. $\Delta(\mathbf{p}) \approx (\Delta_0/p_F^2)(p_x^2 - p_y^2)$ [15], where p_F is the Fermi momentum. This causes the RKKY interaction between localized spins to be highly dependent on which direction they are separated along [9]. Any existing spin-splitting in the superconductor makes the interaction anisotropic in spin space as well [16]. Furthermore, in non-superconducting metals, the RKKY interaction exhibits a decay-oscillation between ferromagnetic and antiferromagnetic as

the separation distance δ between the spins increases. In singlet superconductors, an additional antiferromagnetic coupling appears [9]. If this coupling is sufficiently strong compared to the oscillating contribution discussed above, then the net interaction converges to purely antiferromagnetic beyond some threshold value for δ . This superconductivity-induced coupling can also be long-ranged compared to the conventional RKKY coupling: it decays exponentially over a distance comparable to the superconducting coherence length ξ , rather than exhibiting power-law decay over the Fermi wavelength λ_F as in normal metals. Additional physics comes into play [17, 18] when the RKKY interactions are modified by Yu–Shiba–Rusinov (YSR) bound states [19–21] or by the interfacial bound states that form in d -wave superconductors [22].

Whether the superconducting contribution to the RKKY interaction has a long range or not depends on the magnitude of ξ . Clean BCS superconductors, such as Al, can have very long coherence lengths of order 100 nm. In contrast, high- T_c cuprate superconductors typically have very short coherence lengths of order 5 nm. In addition, the nodal structure of e.g. d -wave superconductors suppresses the superconducting contribution along some axes, since quasiparticles propagating along the nodal directions behave as in a normal metal.

Although the RKKY interaction can be directionally dependent in the presence of unconventional superconducting order, it is still spin-degenerate in singlet superconductors. This means that the interaction between the localized spins takes the form of an effective Heisenberg interaction $\mathcal{H}_{\text{eff}} \sim \mathbf{S}_1 \cdot \mathbf{S}_2$ between the localized spins \mathbf{S}_1 and \mathbf{S}_2 . When spin degeneracy is lifted, e.g. in spin-polarized or spin-orbit-coupled systems, new interactions emerge. For instance, one might find Ising interactions $\mathcal{H}_{\text{eff}} \sim (\mathbf{S}_1 \cdot \mathbf{n})(\mathbf{S}_2 \cdot \mathbf{n})$ or Dzyaloshinskii–Moriya interactions $\mathcal{H}_{\text{eff}} \sim \mathbf{D} \cdot (\mathbf{S}_1 \times \mathbf{S}_2)$, where the vectors \mathbf{n} and \mathbf{D} are related to the symmetries of the underlying material. For this reason, one would expect that spins placed on the surface of a triplet superconductor should exhibit an RKKY interaction that is anisotropic *both* in direction and in spin space. Triplet superconductors are rare, but exist: notable examples include the ferromagnetic superconductors UGe₂ [23] and URhGe [24]. Superconductors that feature spin-polarized Cooper pairs are highly sought after both for use in superconducting spintronics and for their relation to Majorana bound states [25]. To the best of our knowledge, the RKKY interaction in triplet superconductors has not been studied so far.

In this work, we use numerical simulations to investigate the RKKY interaction between localized spins \mathbf{S}_1 and \mathbf{S}_2 on the surface of a p -wave triplet superconductor (see Fig. 1). In addition, we perform analytical calculations based on the Keldysh Green function formalism to verify the generality of our predictions. Due to the rich variety of different spin and orbital structures that these unconventional superconductors can have, we consider a representative selection of different p -wave triplet order parameters (see Table I). We find that in unitary superconductors, the RKKY interaction contains Heisenberg and Ising contributions, whereas in non-unitary superconductors also a Dzyaloshinskii–Moriya term appears. Moreover, the interaction is strongly sensitive to the momentum anisotropy of the p -wave order parameter. Thus, we find that

the RKKY interaction offers information about both the spin and momentum structure of the p -wave triplet state.

II. NUMERICAL CALCULATION

A. Tight-binding model

Consider a square lattice of dimensions $280a \times 40a$, where a is the lattice constant. We take the long axis to be the x axis and the short axis to be the y axis. In the absence of superconductivity, this system is described by the Hamiltonian

$$\mathcal{H}_N = -\mu \sum_{i\sigma} c_{i\sigma}^\dagger c_{i\sigma} - t \sum_{\langle ij \rangle \sigma} c_{i\sigma}^\dagger c_{j\sigma}, \quad (1)$$

where t is the hopping and μ the chemical potential. Henceforth, we set $\mu = -3t$. For an explanation of how the parameters of the tight-binding model were selected, we refer to Section II F. The operators $c_{i\sigma}^\dagger$ and $c_{i\sigma}$ are the usual creation and annihilation operators for spin- σ electrons at lattice site i . We used open boundary conditions (i.e. vacuum interfaces), meaning that the electrons cannot cross the system boundaries.

We then place two classical spins \mathbf{S}_1 and \mathbf{S}_2 at positions \mathbf{R}_1 and \mathbf{R}_2 on the surface of the superconductor, which in the tight-binding model becomes two sites i_1 and i_2 . Each spin interacts with the itinerant electrons via an exchange interaction,

$$\mathcal{H}_F = -\frac{1}{2} \mathcal{J} \sum_{i\sigma\sigma'} \sum_{p=1,2} \delta_{i,i_p} c_{i\sigma}^\dagger (\mathbf{S}_p \cdot \boldsymbol{\sigma})_{\sigma\sigma'} c_{i\sigma'}. \quad (2)$$

where $\boldsymbol{\sigma}$ is the usual Pauli vector and \mathcal{J} is the magnitude of the spin–electron exchange coupling. We set $\mathcal{J} = 3t$ in what follows. We normalize the spins such that $|\mathbf{S}_p| = 1$, which is possible since only the combined magnitude $|\mathcal{J}\mathbf{S}_p|$ enters the numerical model. We place \mathbf{S}_1 at $\mathbf{R}_1 = (140a, 20a)$ and \mathbf{S}_2 at $\mathbf{R}_2 = (140a + \delta, 20a)$, which for small separations δ minimizes the influence of finite-size oscillations. One can then study the RKKY interactions in a normal metal by diagonalizing the Hamiltonian $\mathcal{H}_N + \mathcal{H}_F$ for various spin orientations \mathbf{S}_p and separation distances δ .

To describe superconductors, we in addition have to include the following contribution to the Hamiltonian

$$\mathcal{H}_S = \mathcal{E}_0 - \sum_{ij\sigma} \{ c_{i\sigma}^\dagger [(\Delta_s \delta_{ij} + \Delta_p \cdot \mathbf{v}_{ij}) i \sigma_2]_{\sigma\sigma'} c_{j\sigma'}^\dagger + \text{h.c.} \}, \quad (3)$$

TABLE I. Superconducting order parameters considered herein.

class	d -vector [15]
s -wave singlet	not applicable
p_x -wave triplet	$\mathbf{d}(\mathbf{p}) = \mathbf{e}_z p_x$
p_y -wave triplet	$\mathbf{d}(\mathbf{p}) = \mathbf{e}_z p_y$
chiral p -wave triplet	$\mathbf{d}(\mathbf{p}) = \mathbf{e}_z (p_x + i p_y)$
non-unitary p -wave triplet	$\mathbf{d}(\mathbf{p}) = (1/2)(\mathbf{e}_x + i \mathbf{e}_y)(p_x + i p_y)$

where \mathcal{E}_0 is a constant that depends on Δ_s and Δ_p . We have here introduced the nearest-neighbor vector

$$\mathbf{v}_{ij} \equiv \begin{cases} (\mathbf{r}_j - \mathbf{r}_i)/a & \text{if } |\mathbf{r}_j - \mathbf{r}_i| = a, \\ 0 & \text{otherwise,} \end{cases} \quad (4)$$

where \mathbf{r}_i is the location of site i . Thus, Δ_s describes on-site s -wave singlet pairing, whereas Δ_p is a $3 \times 2 \times 2$ tensor that describes off-site p -wave triplet pairing. The latter is directly related to the standard d -vector parametrization for p -wave triplet order parameters [15], as shown below. Herein, we considered both s -wave and p -wave superconducting states, and the specific d -vectors we used are listed in Table I. In all cases, we set the magnitude of the order parameter to $\Delta_0 = 0.1t$.

B. Superconducting order parameter

There are two common ways to describe the order parameter of a p -wave triplet superconductor [15]. One is a momentum-dependent matrix in spin space,

$$\Delta(\mathbf{p}) = \begin{pmatrix} \Delta_{\uparrow\uparrow}(\mathbf{p}) & \Delta_{\uparrow\downarrow}(\mathbf{p}) \\ \Delta_{\downarrow\uparrow}(\mathbf{p}) & \Delta_{\downarrow\downarrow}(\mathbf{p}) \end{pmatrix}, \quad (5)$$

where the components enter the Fourier-transformed Hamiltonian as terms of the form $\Delta_{\sigma\sigma'}(\mathbf{p})c_{+\mathbf{p},\sigma}^\dagger c_{-\mathbf{p},\sigma'}$. The other approach is to define a vector $\mathbf{d}(\mathbf{p})$ such that

$$\Delta(\mathbf{p}) = (\Delta_0/2p_F)[\mathbf{d}(\mathbf{p}) \cdot \boldsymbol{\sigma}]i\sigma_2, \quad (6)$$

where Δ_0 measures the overall magnitude of the order parameter. The benefit of this approach is that the d -vector transforms as an ordinary vector under spin rotations. The specific choices for $\mathbf{d}(\mathbf{p})$ considered here are listed in Table I.

Numerically, we have used a third parametrization which is closely related to the above d -vector. To motivate this choice, we note that any linear-in-momentum d -vector can be expressed in terms of a 3×3 tensor \mathbf{D} such that

$$\mathbf{d}(\mathbf{p}) = \mathbf{D}\mathbf{p}. \quad (7)$$

When the d -vector is written as in Table I, i.e. with all unit vectors \mathbf{e}_i written to the left of momentum factors p_j , then the corresponding \mathbf{D} -tensor can be obtained by simply replacing the momentum factors $\{p_x, p_y, p_z\}$ by $\{\mathbf{e}_x^T, \mathbf{e}_y^T, \mathbf{e}_z^T\}$. For example, it is straight-forward to verify that $\mathbf{d}(\mathbf{p}) = \mathbf{e}_z(p_x + ip_y)$ can be written $\mathbf{d}(\mathbf{p}) = \mathbf{D}\mathbf{p}$ where $\mathbf{D} = \mathbf{e}_z(\mathbf{e}_x^T + i\mathbf{e}_y^T)$.

Let us now return to the equation for the gap matrix $\Delta(\mathbf{p})$. In terms of the \mathbf{D} -tensor that we introduced above, we see that $\Delta(\mathbf{p}) = (\Delta_0/2p_F)[(\mathbf{D}\mathbf{p})^T \boldsymbol{\sigma}]i\sigma_2 = (\Delta_0/2p_F)[\mathbf{p}^T \mathbf{D}^T \boldsymbol{\sigma}]i\sigma_2$. This motivates the definition of a $3 \times 2 \times 2$ tensor

$$\Delta_p \equiv \frac{1}{2}\Delta_0 \mathbf{D}^T \boldsymbol{\sigma}. \quad (8)$$

In terms of this quantity, the gap matrix for a momentum \mathbf{p} can be trivially calculated as $\Delta(\mathbf{p}) = [\Delta_p \cdot (\mathbf{p}/p_F)]i\sigma_2$.

Now, consider two nearest-neighbor sites i, j on a real-space lattice. We have previously defined a unit vector \mathbf{v}_{ij} which

points along their direction of separation. Electrons that hop between sites i and j will of course have momenta $\mathbf{p} \sim \mathbf{v}_{ij}$, and the real-space order parameter for two nearest-neighbor sites becomes $\Delta_{ij} = (\Delta_p \cdot \mathbf{v}_{ij})i\sigma_2$. This form was used in the tight-binding Hamiltonian in the previous subsection, and highlights that the \mathbf{D} -tensor can be a useful tool to translate general d -vector expressions into real-space order parameters.

C. Calculating the free energy

For a given Hamiltonian $\mathcal{H} = \mathcal{H}_N + \mathcal{H}_F + \mathcal{H}_S$ as described above, we can investigate the RKKY interaction as follows. First, we rewrite the Hamiltonian operator \mathcal{H} in terms of a $4N \times 4N$ Hamiltonian matrix \check{H} as

$$\mathcal{H} = \mathcal{E}_0 + \frac{1}{2}\check{c}^\dagger \check{H} \check{c}, \quad (9)$$

where every creation and annihilation operator on the lattice has been collected into a single $4N$ -element vector as

$$\check{c} \equiv (\hat{c}_1, \dots, \hat{c}_N), \quad \hat{c}_i \equiv (c_{i\uparrow}, c_{i\downarrow}, c_{i\uparrow}^\dagger, c_{i\downarrow}^\dagger). \quad (10)$$

The eigenvalues $\{\epsilon_n\}$ of \mathcal{H} and \check{H} are the same, but the latter is easily determined numerically. For our calculations, we used the SciPy [26] function `scipy.linalg.eigh` with the `evr` driver to obtain the eigenvalue spectrum [27].

Once the eigenvalues are known, the free energy \mathcal{F} follows from the positive eigenvalues:

$$\begin{aligned} \mathcal{F} &= U - TS, \quad U = \mathcal{E}_0 - \frac{1}{2} \sum_{\epsilon_n > 0} \epsilon_n, \\ S &= \sum_{\epsilon_n > 0} \log [1 + \exp(-\epsilon_n/T)]. \end{aligned} \quad (11)$$

This provides a way to numerically calculate the free energy \mathcal{F} from the Hamiltonian \mathcal{H} for each relevant spin configuration. We consider a temperature $T = 0.001t$ far below the critical temperature T_c . As we perform non-selfconsistent calculations, \mathcal{E}_0 is constant and can be neglected when comparing spin configurations. This methodology can nevertheless be used for selfconsistent calculations of the RKKY interaction as well, as reported previously for s -wave singlet superconductors [28].

D. Characterizing the spin-spin interactions

Let us now step away from the microscopic tight-binding Hamiltonian \mathcal{H} for a moment, and consider the general free energy \mathcal{F} of a superconductor interacting with two classical spins. To leading order in \mathbf{S}_1 and \mathbf{S}_2 , we can write

$$\mathcal{F}(\mathbf{S}_1, \mathbf{S}_2) = \mathcal{F}_0 + \boldsymbol{\mu}_1 \cdot \mathbf{S}_1 + \boldsymbol{\mu}_2 \cdot \mathbf{S}_2 + \mathbf{S}_1 \cdot \boldsymbol{\eta} \mathbf{S}_2, \quad (12)$$

where the $\boldsymbol{\mu}_i$ are vectors while $\boldsymbol{\eta}$ is a tensor. We can interpret $\boldsymbol{\mu}_i$ as magnetic interactions between each spin and the superconductor, while $\boldsymbol{\eta}$ is an effective magnetic interaction between the two spins mediated by the superconductor. The remaining

\mathcal{F}_0 contains all contributions that are independent of the spin directions. Note that this includes e.g. the paramagnetic interaction between each spin and a normal metal, which usually only depends on the spin magnitude and not the spin direction. We consider a system with a homogeneous d -vector, and therefore assume that $\boldsymbol{\mu}_1 = \boldsymbol{\mu}_2 \equiv \boldsymbol{\mu}$. The above then becomes

$$\mathcal{F}(\mathbf{S}_1, \mathbf{S}_2) = \mathcal{F}_0 + \boldsymbol{\mu} \cdot (\mathbf{S}_1 + \mathbf{S}_2) + \mathbf{S}_1 \cdot \boldsymbol{\eta} \mathbf{S}_2. \quad (13)$$

Once we have determined the parameters $\{\mathcal{F}_0, \boldsymbol{\mu}, \boldsymbol{\eta}\}$, we could in principle plot the continuous function $\mathcal{F}(\mathbf{S}_1, \mathbf{S}_2)$ to find the ground-state spin configuration. Note that these parameters implicitly depend on the distance δ between the spins.

We now want a protocol to systematically extract $\boldsymbol{\mu}$ and $\boldsymbol{\eta}$ from numerical calculations of $\mathcal{F}(\mathbf{S}_1, \mathbf{S}_2)$. It is convenient to define the following short-hand notation for the free energy,

$$\begin{aligned} \mathcal{F}_{+,+} &\equiv \mathcal{F}(\mathbf{e}_i, \mathbf{e}_j), & \mathcal{F}_{+,-} &\equiv \mathcal{F}(\mathbf{e}_i, -\mathbf{e}_j), \\ \mathcal{F}_{-,+} &\equiv \mathcal{F}(-\mathbf{e}_i, \mathbf{e}_j), & \mathcal{F}_{-,-} &\equiv \mathcal{F}(-\mathbf{e}_i, -\mathbf{e}_j), \end{aligned} \quad (14)$$

where $\mathbf{e}_i, \mathbf{e}_j \in \{\mathbf{e}_x, \mathbf{e}_y, \mathbf{e}_z\}$ are the cardinal unit vectors. Using this notation, we see that we can write each permutation as

$$\begin{aligned} \mathcal{F}_{\pm i, \pm j} &= \mathcal{F}_0 \pm (\mu_i + \mu_j) + \eta_{ij}, \\ \mathcal{F}_{\pm i, \mp j} &= \mathcal{F}_0 \pm (\mu_i - \mu_j) - \eta_{ij}. \end{aligned} \quad (15)$$

From these expressions, it is straight-forward to verify that we can extract all the components of $\boldsymbol{\mu}$ and $\boldsymbol{\eta}$ from

$$\mu_i = \frac{1}{4} [\mathcal{F}_{+,i} - \mathcal{F}_{-,i}], \quad (16)$$

$$\eta_{ij} = \frac{1}{4} [\mathcal{F}_{+,+} - \mathcal{F}_{+,-} - \mathcal{F}_{-,+} + \mathcal{F}_{-,-}] \quad (17)$$

To summarize, we have shown that if we calculate the free energy $\mathcal{F}(\mathbf{S}_1, \mathbf{S}_2)$ for 36 orientations $\mathbf{S}_1, \mathbf{S}_2 \in \{\pm \mathbf{e}_x, \pm \mathbf{e}_y, \pm \mathbf{e}_z\}$ we can fully characterize the leading-order spin interactions.

The elements of $\boldsymbol{\eta}$ can be conveniently parametrized in terms of more conventional magnetic interactions between the spins,

$$\begin{aligned} \mathbf{S}_1 \cdot \boldsymbol{\eta} \mathbf{S}_2 &= J_x S_{1x} S_{2x} + J_y S_{1y} S_{2y} + J_z S_{1z} S_{2z} \\ &+ \mathbf{D} \cdot (\mathbf{S}_1 \times \mathbf{S}_2) + \mathbf{S}_1 \cdot \boldsymbol{\Omega} \mathbf{S}_2, \end{aligned} \quad (18)$$

where J_n are exchange interactions (Heisenberg or Ising), \mathbf{D} is an effective Dzyaloshinskii–Moriya interaction (DMI), while $\boldsymbol{\Omega}$ captures any remaining contributions from $\boldsymbol{\eta}$. In all our simulations—including the s -wave and p -wave results presented here, and some d -wave and $d + is$ -wave results not shown here—we have found $\boldsymbol{\Omega} = 0$ within numerical accuracy. Moreover, in the analytical calculations, we have not identified any term that can not be parametrized using only J_n and \mathbf{D} . For these reasons, we will from here on set $\boldsymbol{\Omega} = 0$.

Explicitly writing out each of the J_n and \mathbf{D} terms, we see that these can be written in terms of the following $\boldsymbol{\eta}$ tensor,

$$\boldsymbol{\eta} = \begin{pmatrix} J_x & +D_z & -D_y \\ -D_z & J_y & +D_x \\ +D_y & -D_x & J_z \end{pmatrix}. \quad (19)$$

Thus, for a system with only the contributions above, we have

$$J_x = \eta_{xx}, \quad D_x = \frac{1}{2}(\eta_{yz} - \eta_{zy}), \quad (20)$$

$$J_y = \eta_{yy}, \quad D_y = \frac{1}{2}(\eta_{zx} - \eta_{xz}), \quad (21)$$

$$J_z = \eta_{zz}, \quad D_z = \frac{1}{2}(\eta_{xy} - \eta_{yx}). \quad (22)$$

Thus, we can obtain the RKKY parameters $\mathbf{J} = (J_x, J_y, J_z)$ and $\mathbf{D} = (D_x, D_y, D_z)$ directly from the tensor $\boldsymbol{\eta}$ extracted from Eq. (17). Notably, this parametrization lets us describe Heisenberg ($J_x = J_y = J_z$), Ising ($J_x = J_y = 0, J_z \neq 0$), and Dzyaloshinskii–Moriya ($\mathbf{D} \neq 0$) interactions between spins.

E. Determining the magnetic ground state

To leading order in \mathbf{S}_1 and \mathbf{S}_2 , we have shown that the free energy of the system in Fig. 1 can be characterized as

$$\mathcal{F} = \mathcal{F}_0 + \boldsymbol{\mu} \cdot (\mathbf{S}_1 + \mathbf{S}_2) + \mathbf{J} \cdot (\mathbf{S}_1 \circ \mathbf{S}_2) + \mathbf{D} \cdot (\mathbf{S}_1 \times \mathbf{S}_2), \quad (23)$$

where \circ refers to elementwise multiplication of two vectors. Moreover, we have demonstrated how to calculate the parameters of this free energy from numerical simulations. Once these are known, we can determine the preferred orientations of the spins by minimizing \mathcal{F} with respect to \mathbf{S}_1 and \mathbf{S}_2 . In real physical systems, there will likely be additional contributions to the free energy due to e.g. magnetocrystalline anisotropy. Such contributions depend on the specific materials and geometries under consideration, and have been neglected in this study. Moreover, the calculation procedure for $\{\boldsymbol{\mu}, \mathbf{J}, \mathbf{D}\}$ assumes that only linear and bilinear terms in \mathbf{S}_1 and \mathbf{S}_2 exist in the free energy. Higher-order terms in the free energy could therefore affect the numerically obtained values for these parameters.

The mathematical problem we need to solve is a constrained optimization problem. Specifically, we need to minimize \mathcal{F} while ensuring that \mathbf{S}_1 and \mathbf{S}_2 remain unit vectors:

$$\begin{aligned} &\text{minimize} && \mathcal{F}(\mathbf{S}_1, \mathbf{S}_2) \\ &\text{subject to} && |\mathbf{S}_1| = |\mathbf{S}_2| = 1. \end{aligned} \quad (24)$$

To solve this numerically, we first convert it to an unconstrained optimization problem. This can be done by incorporating the constraints into the objective function as penalty terms:

$$\mathcal{G}(\mathbf{S}_1, \mathbf{S}_2) = \mathcal{F}(\mathbf{S}_1, \mathbf{S}_2) + \lambda |\mathbf{S}_1|^2 - 1|^2 + \lambda |\mathbf{S}_2|^2 - 1|^2. \quad (25)$$

For suitably large penalties λ , the constraints are automatically satisfied as the penalized objective function \mathcal{G} is minimized.

Non-convex optimization requires an initial guess for the variables \mathbf{S}_1 and \mathbf{S}_2 , and can identify different local minima in \mathcal{F} depending on this guess. To find the *global* energy minimum (or minima), we therefore have to repeat the optimization procedure with different starting points and compare the final results. In our case, we used as initial guesses

$$\mathbf{S}_1, \mathbf{S}_2 \in \left\{ \cos \theta \mathbf{e}_x + \sin \theta \mathbf{e}_z \mid \theta \in \{0^\circ, 45^\circ, \dots, 360^\circ\} \right\}, \quad (26)$$

which produces uniformly spaced starting points in the xz plane. In our study, it is sufficient to focus on the xz plane since all d -vectors listed in Table I were found to produce $J_x = J_y$, $\mu \sim e_z$, and $D \sim e_z$. Under these conditions, the free energy is invariant under spin rotations in the xy plane.

For each initial guess, we minimized $\mathcal{G}(S_1, S_2)$ using the SciPy [26] function `scipy.optimize.minimize` with the Powell backend. The penalty $\lambda \in \{10^0, 10^1, \dots, 10^6\}$ was increased exponentially between successive calls to the optimizer; this eased the convergence of initial iterations, but strongly enforced the constraints in final iterations. After the final call to the optimizer, we saved the optimized spin configuration (S_1, S_2) and free energy $\mathcal{F}(S_1, S_2)$. After an independent optimization for each initial guess, the real ground state was taken to be the optimization result with the lowest value for \mathcal{F} .

We have verified that for systems with known ground states (e.g. systems with pure Heisenberg, Ising, or Dzyaloshinskii–Moriya interactions), the procedure above reproduces the known ground states. The procedure was then applied to the numerically calculated $\mathcal{F}(S_1, S_2)$ for p -wave triplet superconductors with various separations δ between the spins.

F. Parameter study

When a spin S is placed on the surface of a superconductor, a Yu–Shiba–Rusinov (YSR) bound state can emerge [19–21]. This state manifests as a peak within the subgap local density of states (LDOS). The amplitude of this peak oscillates and decays with increased distance from the spin. When these bound states (i) have a high amplitude and (ii) are visible farther from the spin site, we can infer that the spin must more strongly affect the material on which it is placed. Intuitively, we would also expect RKKY interactions between spins to be enhanced in this limit. It is much more computationally efficient to look for YSR signatures (LDOS calculations) than to determine RKKY interactions (free energy calculations). We therefore used YSR signatures as a proxy to determine optimal parameters for our RKKY calculations. Our methodology for efficient LDOS computation on large lattices is detailed in Appendix A.

We set the superconducting gap $\Delta_0 = 0.1t$. Lower values would be more realistic for typical low-temperature superconductors; however, too small values make it challenging to pick out the YSR state amid subgap peaks caused by finite size effects. One possible remedy is to consider extremely large lattices, thus abating the finite size effects. However, the required system sizes quickly become computationally infeasible. Our choice $\Delta_0 = 0.1t$ strikes a balance between realism and feasibility, as is common in numerical treatments of superconductivity based on tight-binding models.

For the exchange coupling between each classical spin and the superconductor, a moderately large value $J = 3t$ was chosen. A significant ratio $J/\Delta_0 = 30$ as chosen here is not uncommon; for instance, Ref. [29] estimated a ratio of over a thousand for Mn adatoms on an Nb superconductor. In practice, this parameter J can vary significantly depending on the specific materials used in an experiment, and the YSR signatures become clearer the larger this parameter grows. Notably, some experimental

setups also permit in-situ tuning of its precise value [30].

Lastly, a chemical potential $\mu \approx -3t$ was deemed optimal for obtaining pronounced YSR signatures. As $\mu \rightarrow -4t$ the amplitude of the YSR state becomes negligible, whereas for $\mu \rightarrow 0$ the YSR state becomes so strongly localized that it is only clearly visible from the nearest-neighbor site. The value $\mu = -3t$ strikes a good compromise, where a clear LDOS subgap peak is visible from several lattice sites away.

After obtaining $\{\Delta_0 = 0.1t, J = 3t, \mu = -3t\}$ from studying YSR states in p -wave superconductors, we proceeded to study RKKY interactions with the same parameters as a basis. We believe that the general conclusions of our study are robust the specific system parameters—especially since the same qualitative contributions were also derived analytically in Section III without reference to these particular system parameters.

III. ANALYTICAL CALCULATION

Consider a homogeneous superconductor described by a 4×4 Green function $\hat{G}^R(\mathbf{p}, \omega)$ in Nambu \otimes spin space, where \mathbf{p} and ω are momentum and energy variables. As in the numerical case, we then place two classical spins $S_{1,2}$ at coordinates $\mathbf{R}_{1,2}$, where each spin couples to the superconductor via local exchange interactions with strength \mathcal{J} . Leading-order perturbation theory then shows that the equilibrium energy of the system acquires a term

$$E_{\text{RKKY}} = \frac{1}{4}\pi\mathcal{J}^2 \text{Im} \int d\omega \tanh(\omega/2T) \times \int d\mathbf{p}_1 \int d\mathbf{p}_2 e^{-i(\mathbf{p}_2 - \mathbf{p}_1) \cdot (\mathbf{R}_2 - \mathbf{R}_1)} \times \text{Tr} \left\{ (S_1 \cdot \hat{\sigma}) \hat{G}^R(\mathbf{p}_1, \omega) (S_2 \cdot \hat{\sigma}) \hat{G}^R(\mathbf{p}_2, \omega) \right\}, \quad (27)$$

where $\hat{\sigma} = \text{diag}(\sigma, \sigma^*)$. Although this is a well-established equation in the literature (see e.g. Refs. [5, 31, 32]), we provide a complete derivation in Appendix B. The RKKY interaction can then be understood as a reorientation of S_1 and S_2 in an attempt to minimize this term in the system's energy.

Consider now a p -wave triplet superconductor. The Nambu-space structure of its retarded Green function can be written

$$\hat{G}^R(\mathbf{p}, \omega) = \begin{pmatrix} G(\mathbf{p}, \omega) & F(\mathbf{p}, \omega) \\ \tilde{F}(\mathbf{p}, \omega) & \tilde{G}(\mathbf{p}, \omega) \end{pmatrix}, \quad (28)$$

where the normal component G describes quasiparticles, the anomalous component F describes Cooper pairs, and $\tilde{X}(\mathbf{p}, \omega) \equiv X^*(-\mathbf{p}, -\omega)$. Substituting this into the equation for E_{RKKY} , one can show that (see Appendix C)

$$E_{\text{RKKY}} = \frac{1}{2}\pi\mathcal{J}^2 \text{Im} \int d\mathbf{p}_1 \int d\mathbf{p}_2 e^{-i(\mathbf{p}_2 - \mathbf{p}_1) \cdot (\mathbf{R}_2 - \mathbf{R}_1)} \times \int d\omega \tanh(\omega/2T) (\mathcal{G} + \mathcal{F}), \quad (29)$$

where the contributions from quasiparticles and Cooper pairs

are given by the two amplitudes

$$\mathcal{G} = \text{Tr}[(\mathbf{S}_1 \cdot \boldsymbol{\sigma})G(\mathbf{p}_1, \omega)(\mathbf{S}_2 \cdot \boldsymbol{\sigma})G(\mathbf{p}_2, \omega)], \quad (30)$$

$$\mathcal{F} = \text{Tr}[(\mathbf{S}_1 \cdot \boldsymbol{\sigma})F(\mathbf{p}_1, \omega)(\mathbf{S}_2 \cdot \boldsymbol{\sigma}^*)\tilde{F}(\mathbf{p}_2, \omega)]. \quad (31)$$

In non-superconducting metals, \mathcal{G} typically gives rise to a Heisenberg interaction $\sim \mathbf{S}_1 \cdot \mathbf{S}_2$ between the two spins [1–3], while $\mathcal{F} = 0$ in the absence of superconductivity. In spin-orbit-coupled materials, \mathcal{G} can also give rise to Ising $\sim (\mathbf{S}_1 \cdot \mathbf{n})(\mathbf{S}_2 \cdot \mathbf{n})$ and Dzyaloshinskii–Moriya $\sim \mathbf{D} \cdot (\mathbf{S}_1 \times \mathbf{S}_2)$ interactions [5, 32].

Below the superconducting critical temperature, both \mathcal{G} and \mathcal{F} change. For the quasiparticle contribution \mathcal{G} , this is because a momentum-dependent gap $|\Delta(\mathbf{p})|$ opens in the excitation spectrum in the superconducting state, which modulates this Heisenberg contribution. The other contribution \mathcal{F} is naturally only nonzero in the presence of superconductivity, and can contain qualitatively new RKKY contributions that are sensitive to the symmetries of the order parameter. Below, we focus on the latter contribution. Substituting the d -vector parametrization $F(\mathbf{p}, \omega) = [\mathbf{d}(\mathbf{p}, \omega) \cdot \boldsymbol{\sigma}]i\sigma_2$ into the definition of \mathcal{F} , a direct calculation shows that (see Appendix C)

$$\begin{aligned} \mathcal{F} = & -4 [\mathbf{S}_1 \cdot \mathbf{d}(\mathbf{p}_1, \omega)][\mathbf{S}_2 \cdot \tilde{\mathbf{d}}(\mathbf{p}_2, \omega)] \\ & + 2 [\mathbf{d}(\mathbf{p}_1, \omega) \cdot \tilde{\mathbf{d}}(\mathbf{p}_2, \omega)][\mathbf{S}_1 \cdot \mathbf{S}_2] \\ & + 2 [\mathbf{d}(\mathbf{p}_1, \omega) \times \tilde{\mathbf{d}}(\mathbf{p}_2, \omega)] \cdot [\mathbf{S}_1 \times \mathbf{S}_2]. \end{aligned} \quad (32)$$

We here use a d -vector parametrization of the anomalous Green function $F(\mathbf{p}, \omega)$ as opposed to the order parameter $\Delta(\mathbf{p})$. These quantities are usually related by a distribution-weighted energy integration, and thus the $\mathbf{d}(\mathbf{p}, \omega)$ considered analytically and $\mathbf{d}(\mathbf{p})$ considered numerically are closely related. Moreover, one does not necessarily require an intrinsic non-unitary triplet superconductor to access such a quantum state. This type of superconductivity is also known to arise in hybrid structures comprised of ferromagnets and conventional superconductors [33–36]. This could then serve as an alternative, and perhaps experimentally more accessible, arena for probing the RKKY interaction mediated by a non-unitary superconducting state.

The first term is an Ising interaction between \mathbf{S}_1 and \mathbf{S}_2 , where only spin components along some special axis \mathbf{n} couple: $E_{\text{RKKY}} \sim (\mathbf{S}_1 \cdot \mathbf{n})(\mathbf{S}_2 \cdot \mathbf{n})$. For a concrete example, consider the p_x -wave superconductor $\mathbf{d}(\mathbf{p}, \omega) = d(\omega)p_x\mathbf{e}_z$. The Ising term is then proportional to $p_{1x}p_{2x}S_{1z}S_{2z}$, such that (i) only the z -components of the spins couple and (ii) there is a strong directional anisotropy due to the presence of p_x factors.

The second term is a superconductivity-mediated Heisenberg contribution: $E_{\text{RKKY}} \sim \mathbf{S}_1 \cdot \mathbf{S}_2$. Similar contributions appear in both s -wave and d -wave singlet superconductors [9]. However, the momentum symmetry differs for p -wave superconductors as the integrand $\sim \mathbf{d}(\mathbf{p}_1, \omega) \cdot \mathbf{d}^*(-\mathbf{p}_2, -\omega) e^{-i(\mathbf{p}_2 - \mathbf{p}_1) \cdot (\mathbf{R}_2 - \mathbf{R}_1)}$ still contains the strongly anisotropic factors $\mathbf{d}(\mathbf{p}, \omega)$.

Finally, consider the third term. This term is non-zero in non-unitary superconductors where $\mathbf{d} \times \mathbf{d}^*$ is nonzero [15]. For example, it is finite in chiral non-unitary superconductors with the order parameter $\mathbf{d}(\mathbf{p}, \omega) = d(\omega)(p_x + ip_y)(\mathbf{e}_x + i\mathbf{e}_y)$, where we see that $\mathbf{d} \times \tilde{\mathbf{d}} \sim \mathbf{d} \times \mathbf{d}^* \sim \mathbf{e}_z$. This takes the form of an effective Dzyaloshinskii–Moriya interaction [37, 38] $E_{\text{RKKY}} \sim \mathbf{D} \cdot (\mathbf{S}_1 \times \mathbf{S}_2)$ which prefers to misalign spins, where

the DMI vector is given by $\mathbf{D} \sim \mathbf{d} \times \mathbf{d}^*$. RKKY interactions of this form have previously been shown to arise in materials with Rashba spin-orbit coupling; but to our knowledge, it has not before been reported to originate purely from superconductivity.

To summarize, we have analytically shown that when two spins \mathbf{S}_1 and \mathbf{S}_2 are placed in contact with a triplet p -wave superconductor, the Cooper pairs can mediate three different types of RKKY interactions between the spins:

- (i) Ising-like: $E_{\text{RKKY}} \sim (\mathbf{S}_1 \cdot \mathbf{n})(\mathbf{S}_2 \cdot \mathbf{n})$;
- (ii) Heisenberg-like: $E_{\text{RKKY}} \sim (\mathbf{S}_1 \cdot \mathbf{S}_2)$;
- (iii) DMI-like: $E_{\text{RKKY}} \sim \mathbf{D} \cdot (\mathbf{S}_1 \times \mathbf{S}_2)$.

Here, $\mathbf{n} \sim \mathbf{d}$ and $\mathbf{D} \sim \mathbf{d} \times \mathbf{d}^*$ depend sensitively on the spin symmetries of the triplet superconducting order parameter. In addition, all these interactions depend on the momentum anisotropy in $\mathbf{d}(\mathbf{p}, \omega)$. This shows that the RKKY interaction can be used as a probe for both the spin and momentum symmetries of the underlying triplet p -wave order parameter. As we will see in the next section, these analytical predictions fit very well with the numerical results obtained using the methodology presented in the previous section.

IV. RESULTS AND DISCUSSION

The simplest p -wave triplet state is arguably the p_x -wave state described by $\mathbf{d}(\mathbf{p}) = p_x\mathbf{e}_z$. In this state, the superconducting gap is highly anisotropic in momentum space:

$$|\Delta(\mathbf{p})| \rightarrow \begin{cases} \Delta_0 & \text{for } \mathbf{p} \rightarrow \pm p_F \mathbf{e}_x, \\ 0 & \text{for } \mathbf{p} \rightarrow \pm p_F \mathbf{e}_y. \end{cases} \quad (33)$$

Thus, when two spins \mathbf{S}_1 and \mathbf{S}_2 are displaced along the x axis on the surface of this superconductor (see Fig. 1), quasiparticles traveling directly from one spin to the other would “see” a full gap at the Fermi level. This situation is qualitatively similar to in an s -wave superconductor. On the other hand, if the spins are displaced along the y axis, quasiparticles would see no gap and thus behave similarly to in a normal metal. In this case, rotating the whole physical system by 90° in the xy plane would yield a p_y wave superconductor with spins separated along the x axis. We have opted to study the latter case in this paper.

Using the methodology presented in Section II, we have numerically calculated the RKKY coupling J_z between two spins when placed on p_x and p_y wave superconductors. This coupling corresponds to an effective interaction $J_z S_{1z} S_{2z}$ in the free energy of the system. In Fig. 2, these results are compared to the corresponding RKKY interactions in normal metals and s -wave superconductors. In line with the argument above, we find that the results for s -wave and p_x -wave superconductors are quite similar, whereas the results for normal metals and p_y -wave superconductors are nearly indistinguishable.

In normal metals and singlet superconductors, the RKKY interactions between spins are of the Heisenberg type, so the coefficients $J_x = J_y = J_z$ are all equal. In triplet superconductors, the net spins of the Cooper pairs can lead to different RKKY

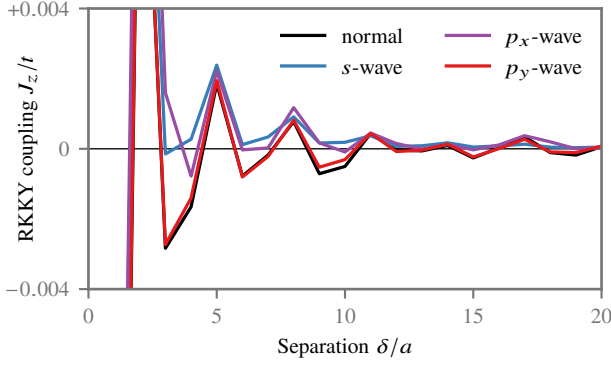


FIG. 2. Comparison of the RKKY coupling J_z for the simplest p -wave order parameters with normal metals and s -wave superconductors. Note that the results for the p_x -wave order parameter are qualitatively similar to those for the s -wave order parameter, whereas the results for the p_y -wave order parameter are nearly indistinguishable from the normal metal results.

interactions for different spin projections. Since all states considered herein are invariant under rotations in the xy plane, we can parametrize this as $\mathcal{F} = \bar{J}(\mathbf{S}_1 \cdot \mathbf{S}_2) + \delta J(\mathbf{S}_1 \cdot \mathbf{e}_z)(\mathbf{S}_2 \cdot \mathbf{e}_z)$, where \bar{J} is the Heisenberg part and δJ the Ising part. Compared to the formulation $\mathcal{F} = \sum_n J_n S_{1n} S_{2n}$ of the free energy, this parametrization corresponds to $J_x = J_y = \bar{J}$ and $J_z = \bar{J} + \delta J$.

In Fig. 3, we show the numerical results for \bar{J} and δJ for each p -wave triplet order parameter listed in Table I. For the p_y -wave state [Fig. 3(b)], the RKKY interaction is nearly purely Heisenberg-like, similarly to what one would observe in a normal metal. What is not so visible in the plot is that there exists a very weak Ising term δJ as well, which is consistently negative (ferromagnetic). This contribution is however two orders of magnitude smaller than the Heisenberg contribution, and it is therefore unclear to what extent it would be experimentally observable. For the p_x -wave state [Fig. 3(a)], the Ising contribution becomes much stronger: In fact, it is the dominant contribution to \mathcal{F} for most values of δ . The Heisenberg contribution in p_x -wave superconductors looks like a strongly damped version of the interaction in p_y -wave superconductors (and normal metals), whereas the Ising contribution has a bias towards positive (antiferromagnetic) values of δJ . Nearly identical results are found for the chiral p -wave superconductors [Fig. 3(c)]. This makes sense, because the order parameters of p_x -wave and chiral p -wave superconductors look identical for particles traveling along the x axis. The core difference between these two states is that the chiral p -wave state would produce identical results also for spin displacements along the y axis, in contrast to the p_x -wave state discussed above.

Finally, we consider a non-unitary superconductor. Non-unitary superconductors have two crucial differences from the other p -wave triplet states that we study [15]. Firstly, their Cooper pair condensate has a finite spin expectation value $\boldsymbol{\mu} \sim \mathbf{d} \times \mathbf{d}^*$, which can couple magnetically to each individual spin \mathbf{S}_1 and \mathbf{S}_2 . In Fig. 4, we show the numerical results for $\boldsymbol{\mu}$ obtained using the methodology developed in Section II. Secondly, non-unitary superconductors generally

have spin-dependent order parameters: $\Delta_{\uparrow}(\mathbf{p}) \neq \Delta_{\downarrow}(\mathbf{p})$. For the particular non-unitary state considered here, all relevant momenta $\mathbf{p} = p_x \mathbf{e}_x + p_y \mathbf{e}_y$ yield a full gap $|\Delta_{\uparrow}| = \Delta_0$ in one spin band and no gap $|\Delta_{\downarrow}| = 0$ in the other. In this case, both Cooper pairs and low-energy quasiparticles can always contribute to the RKKY interaction—regardless of what direction in the xy plane the spins are separated along. The consequence of this is visible in Fig. 3(d): The Heisenberg interaction is very similar to in a normal metal due to the quasiparticle contribution, but there is also a significant Ising interaction due to the Cooper-pair contribution. One might however ask why the Ising contribution appears to be negative (ferromagnetic), as opposed to e.g. the chiral p -wave case where a positive (antiferromagnetic) value was found. This is simply a consequence of our parametrization. When comparing the chiral state $\mathbf{d}(\mathbf{p}) = (p_x + ip_y)\mathbf{e}_z$ to the non-unitary state $\mathbf{d}(\mathbf{p}) = (1/2)(p_x + ip_y)(\mathbf{e}_x + \mathbf{e}_z)$, we might expect that a positive Ising term along the z axis in the former case would correspond to positive Ising terms in along the x and y axes in the latter case. Positive Ising terms along the x and y axes can equivalently be described as a negative Ising term along the z axis, with a corresponding shift of the Heisenberg term [39]. This is precisely what we find in our numerical results.

In Section III, we showed analytically that non-unitary superconductors can mediate effective Dzyaloshinskii–Moriya interactions $\sim \mathbf{D} \cdot (\mathbf{S}_1 \times \mathbf{S}_2)$ between spins, where the DMI vector $\mathbf{D} \sim \mathbf{d} \times \mathbf{d}^* \sim \boldsymbol{\mu}$ is proportional to the spin expectation value of the Cooper pair condensate. Moreover, in Section II, we showed how this DMI vector could be extracted from numerical simulations. The results of this procedure are shown in Fig. 5. In line with the theoretical predictions, the numerical simulations confirm the presence of a DMI vector $\mathbf{D} \sim \boldsymbol{\mu}$. Similarly to the usual RKKY interaction, this DMI contribution oscillates and decays as a function of the separation distance δ between the two spins. For this particular non-unitary state, the DMI prefers non-collinear spin orientations in the xy plane.

In practice, the DMI vector obtained here is likely too small to be experimentally observable. This is made clearer if one plots the magnitudes of the different terms in the free energy as a function of separation distance δ (see Fig. 6). This shows that the DMI coefficient remains two orders of magnitude smaller than the other contributions to the free energy for all separation distances. Whether the dominant contribution is an RKKY interaction or a magnetic interaction depends on the separation distance between the two spins. Although the DMI interaction is too small to be observable for the parameter space we have explored, its existence motivates further studies of non-unitary superconductivity (either intrinsic or arising in hybrid structures) where it could be possible to find ways to increase the magnitude of the DMI interaction.

In Fig. 7, we plot the ground-state spin configuration for the various \mathbf{d} -vectors presented in Table I. These configurations were obtained using the methodology presented in Section II E. In normal metals and s -wave superconductors (not shown), the RKKY interaction oscillates between ferromagnetic and antiferromagnetic as a function of δ . However, since it is a pure Heisenberg interaction $\sim \mathbf{S}_1 \cdot \mathbf{S}_2$, it is *completely* degenerate with respect to simultaneous spin rotations of \mathbf{S}_1 and \mathbf{S}_2 . (Note

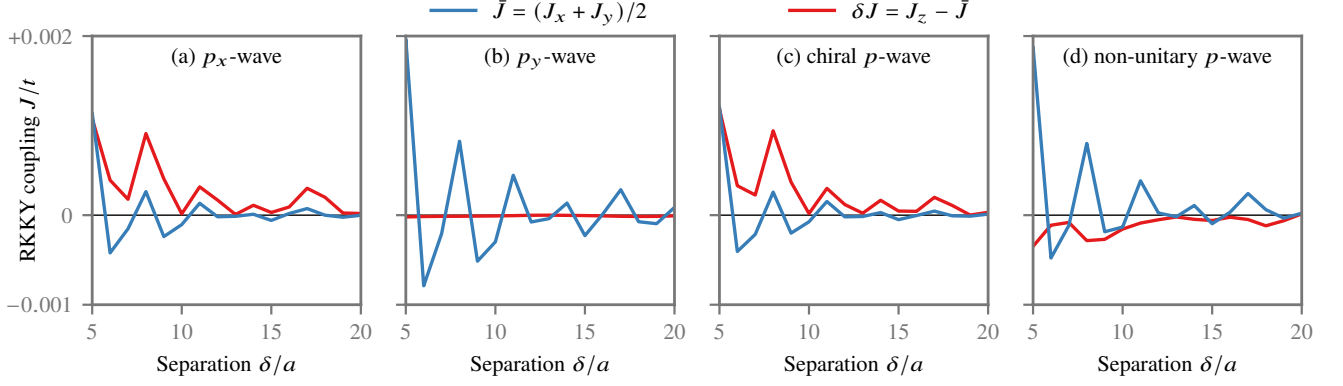


FIG. 3. Comparison of the different RKKY interaction components $\{J_x, J_y, J_z\}$ for the considered p -wave order parameters. The results are clearly sensitive to the spin part of the \mathbf{d} vector: e.g. for $\mathbf{d} = \mathbf{e}_z p_x$ the interaction is clearly more antiferromagnetic for J_z than for J_x, J_y . In the case of the non-unitary superconductor, the interaction is more antiferromagnetic for *both* the x and y directions as compared to the z direction, which in our parametrization leads to a negative value for δJ .

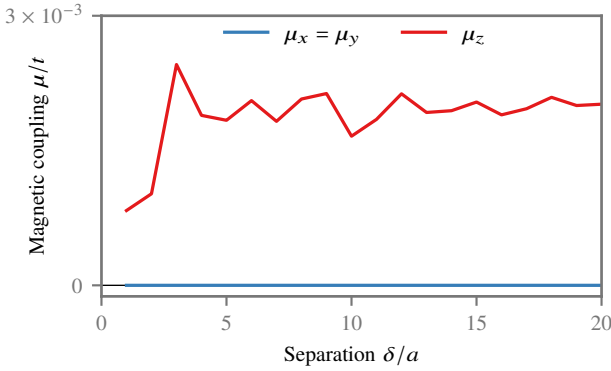


FIG. 4. Magnetic interaction μ between a non-unitary superconductor and each impurity. For this particular system, a magnetic coupling $\mu \approx 0.002te_z$ was found which does not sensitively depend on the distance between the impurities. We generally found $\mu = 0$ for unitary superconducting orders—including states that break time reversal symmetry, such as chiral p -wave and $d + is$ -wave superconductors.

however that we have neglected magnetic anisotropy herein, which could break this degeneracy in real systems.) With a p_y -wave order parameter, the situation is *nearly* the same as in a normal metal: The dominant contribution to the RKKY interaction is still the Heisenberg term. However, we also find a very small ferromagnetic Ising term $\sim -(\mathbf{S}_1 \cdot \mathbf{e}_z)(\mathbf{S}_2 \cdot \mathbf{e}_z)$. This term breaks the rotational symmetry in the xz plane, and makes the system prefer ferromagnetic orientation along the z axis but antiferromagnetic orientation along the x axis. Given the small magnitude of this Ising contribution for our parameter choices, this effect may not be visible in experiments.

Next, consider the p_x -wave order parameter. The results are then exactly opposite from the p_y -wave case: The system oscillates between ferromagnetic ordering along the x axis and antiferromagnetic ordering along the z axis. However, the Ising interaction is in this case the same order of magnitude as the Heisenberg interaction (see Fig. 3). We therefore expect this

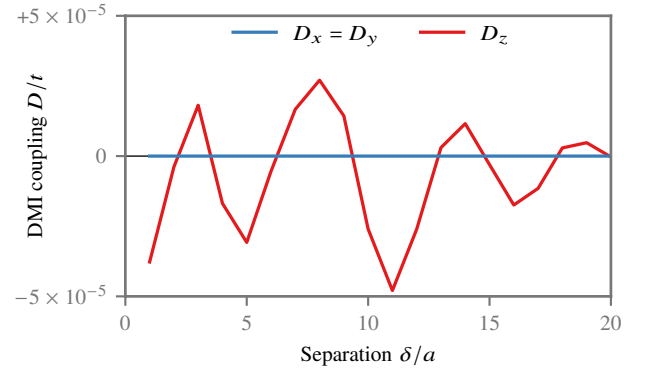


FIG. 5. DMI-like interaction $\mathbf{D} \cdot (\mathbf{S}_1 \times \mathbf{S}_2)$ for the non-unitary superconductor. Similarly to the usual RKKY interaction, it oscillates as a function of the distance between the impurities. Similarly to the usual exchange-like RKKY interaction, we find that this new contribution oscillates between positive and negative values as a function of the distance between the two spins. We found no such interaction in unitary superconductors—including chiral p -wave and $d + is$ -wave superconductors, which also break time reversal symmetry.

oscillation between in-plane and out-of-plane spin ordering to be much more robust than for the p_y -wave order parameter, and to be experimentally observable. The configurations we obtain for chiral p -wave and p_x wave orders are identical—which we could expect as these materials look the same for quasiparticles propagating between \mathbf{S}_1 and \mathbf{S}_2 (i.e. along the x axis).

Finally, let us discuss the results for the non-unitary superconductor. One might expect behavior reminiscent of the p_y -wave superconductor since both of these materials have available zero-energy quasiparticle states. Specifically, the non-unitary superconductor we considered has a gap in only one spin band, whereas the p_y wave superconductor has no gap for propagation along the x axis. However, there are some important differences between these systems, which arise from the magnetization $\mu \sim \mathbf{d} \times \mathbf{d}^*$ in the non-unitary superconduc-

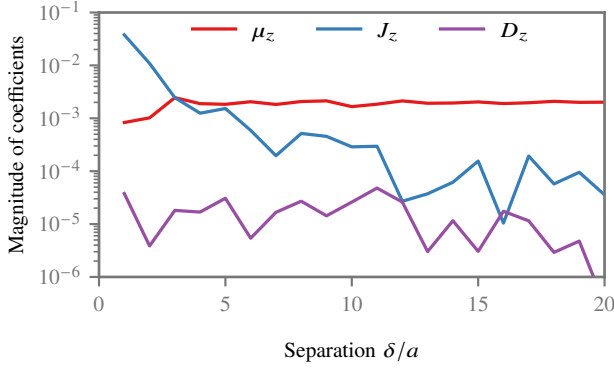


FIG. 6. Magnitude of the magnetic interaction $|\mu_z|$, Ising interaction $|J_z|$, and Dzyaloshinskii–Moriya interaction $|D_z|$ for the non-unitary superconductor (in units of t). For the parameters we have considered, the DMI contribution is found to be roughly two orders of magnitude lower than the other contributions to the free energy.

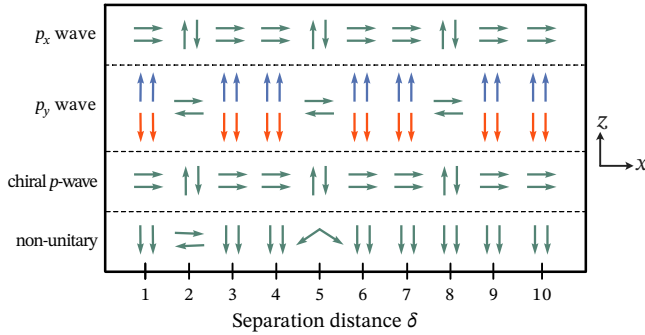


FIG. 7. Ground-state orientation of the two spins S_1 and S_2 in Fig. 1 for the p -wave triplet order parameters in Table I. For values of δ where a single ground state is found, we plot S_1 and S_2 as two green arrows. When two degenerate solutions exist, we plot one set of solutions as blue arrows and the other as orange arrows. We here focus on solutions in the xz plane; the degenerate solutions that can be obtained by spin rotation in the xy plane are not shown. Note that the numerical results indicate a negligible DMI coefficient D compared to the other terms in the free energy; in systems where this is not the case, also the y components of the spins would be important.

tor. Firstly, μ breaks the symmetry between the $+z$ and $-z$ axes, so in the ferromagnetic state the spins always align along the $-z$ axis. Secondly, this magnetization becomes the dominant energy scale for long separation distances δ , and thus the oscillation between ferromagnetic and antiferromagnetic states stops beyond some distance. Finally, when the spins prefer antiferromagnetic alignment along the x axis, the $\mu_z(S_{1z} + S_{2z})$ interaction yields an additional ferromagnetic coupling along the z axis. This produces non-collinearity. Specifically, for $\delta = 2a$ and $\delta = 5a$, respectively, the precise angle between the two spins in the ground state is 175.3° and 113.1° . If the DMI vector had been larger, an additional non-collinearity could have been found in the xy plane. However, in our particular simulation results, this effect was found to be negligible.

V. CONCLUSION

We have studied the RKKY interactions in p -wave triplet superconductors numerically and analytically. Similarly to singlet superconductors, we find that the momentum dependence of the superconducting gap $|\Delta(\mathbf{p})|$ strongly affects the RKKY interaction. However, in triplet superconductors the order parameter also develops a spin structure. We have shown that this leads to new Ising-like and Dzyaloshinskii–Moriya-like RKKY interactions between spins placed on the surface of the superconductor. The Ising contribution is generally large, whereas the DMI contribution was zero for unitary superconductors and small but finite for non-unitary superconductors. An interesting venue for further research would be to determine whether the DMI contribution could be enhanced in other physical setups, as the effect of the DMI vector on the magnetic ground state was found to be negligible for the parameters studied herein. Despite a negligible DMI effect, we find that a non-collinear spin configuration arises in non-unitary triplet superconductors due to a combination of antiferromagnetic in-plane RKKY interactions and ferromagnetic out-of-plane interactions with the Cooper pair condensate. Our results suggest that the RKKY interaction in p -wave triplet superconductors can be used as a probe for both the spin and momentum symmetries of the superconducting order parameter.

ACKNOWLEDGMENTS

This work was supported by the Research Council of Norway through Grant No. 323766 and its Centres of Excellence funding scheme Grant No. 262633 “QuSpin.” This work was also supported by JSPS KAKENHI Grant Number JP30578216 and the JSPS-EPSRC Core-to-Core program “Oxide Superspin”. The numerical calculations were performed on resources provided by Sigma2—the National Infrastructure for High Performance Computing and Data Storage in Norway, project NN9577K.

Appendix A: Efficient calculation of the LDOS

We now describe the calculation procedure for the local density of states (LDOS). One way to define the Green function is as the *resolvent* of the Hamiltonian [40–42]. Given the $4N \times 4N$ Hamiltonian matrix \tilde{H} introduced in Section II A, the Green function matrix on the lattice is then given by

$$[(\omega + i\eta)\tilde{I} - \tilde{H}]\tilde{G}^R(\omega) = \tilde{I}, \quad (\text{A1})$$

where \tilde{I} is an identity matrix, ω is the energy, and $\eta \rightarrow 0^+$ yields the retarded Green function. In practice, we let η go to a small but finite value; this broadens the δ -function peaks in the LDOS to finite-width Lorentzians, which are easier to evaluate numerically. From the diagonal elements of this $4N \times 4N$ Green function matrix, we can then obtain the spin-resolved

LDOS $N_{i\sigma}$ at every lattice site i [41, 42]:

$$N_{i\uparrow}(+\omega) = -\frac{1}{\pi} \text{Im}[G_{4i+1,4i+1}^R(\omega)], \quad (\text{A2})$$

$$N_{i\downarrow}(+\omega) = -\frac{1}{\pi} \text{Im}[G_{4i+2,4i+2}^R(\omega)], \quad (\text{A3})$$

$$N_{i\uparrow}(-\omega) = -\frac{1}{\pi} \text{Im}[G_{4i+3,4i+3}^R(\omega)], \quad (\text{A4})$$

$$N_{i\downarrow}(-\omega) = -\frac{1}{\pi} \text{Im}[G_{4i+4,4i+4}^R(\omega)], \quad (\text{A5})$$

Since the Green function contains information about both electrons and holes when we use the Nambu-space formulation, we only need to determine the Green function for $\omega \geq 0$ to plot the LDOS for all ω . Moreover, to study YSR states, calculating the LDOS for $\omega \in [0, \Delta_0]$ is usually sufficient.

The most straight-forward way to solve Eq. (A1) for the Green function is direct matrix inversion: $\check{G}^R(\omega) = [(\omega + i\eta)\check{I} - \check{H}]^{-1}$. In practice, this is prohibitively expensive numerics for large systems. Instead, let us exploit the property that we only require the Green function elements $G_{n,n}^R$ for a few specific indices n in order to determine the LDOS at one specific lattice site i . If we split the Green function matrix $\check{G}^R = [\check{x}_1 \cdots \check{x}_{4N}]$ into column vectors and the identity matrix $\check{I} = [\check{e}_1 \cdots \check{e}_{4N}]$ into unit vectors, then Eq. (A1) can equivalently be written

$$\check{A}(\omega) \check{x}_n(\omega) = \check{e}_n, \quad (\text{A6})$$

where $\check{A}(\omega) \equiv (\omega + i\eta)\check{I} - \check{H}$. This is a standard linear system of equations, which can be solved very efficiently using e.g. the SciPy [26] function `scipy.sparse.linalg.spsolve` if \check{A} and \check{e}_n are stored as sparse matrices. Once these equations have been solved for $n \in \{4i+1, \dots, 4i+4\}$, the LDOS at lattice site i is easily found from the result vectors:

$$N_{i\uparrow}(+\omega) = -\frac{1}{\pi} \text{Im}[\check{e}_{4i+1} \cdot \check{x}_{4i+1}(\omega)], \quad (\text{A7})$$

$$N_{i\downarrow}(+\omega) = -\frac{1}{\pi} \text{Im}[\check{e}_{4i+2} \cdot \check{x}_{4i+2}(\omega)], \quad (\text{A8})$$

$$N_{i\uparrow}(-\omega) = -\frac{1}{\pi} \text{Im}[\check{e}_{4i+3} \cdot \check{x}_{4i+3}(\omega)], \quad (\text{A9})$$

$$N_{i\downarrow}(-\omega) = -\frac{1}{\pi} \text{Im}[\check{e}_{4i+4} \cdot \check{x}_{4i+4}(\omega)]. \quad (\text{A10})$$

This approach provides an $\mathcal{O}(N)$ computational speedup over a full matrix inversion $\check{G}^R(\omega) = \check{A}^{-1}(\omega)$, since we now only calculate the specific columns of $\check{G}^R(\omega)$ that are required to evaluate the *local* density of states at one or a few sites. For moderately large lattices (10^4 – 10^5 sites), we found that this approach outperforms direct matrix inversion (as discussed above), matrix diagonalization (the conventional approach), and Chebyshev matrix expansion [42, 43].

The approach above is inspired by Nagai et al. [41]. Their algorithm is likely more efficient, as it re-uses results between different ω values, whereas in our case the calculation at each ω is independent. The procedure we used is however much simpler, as it can be implemented in few lines of code that leverages standard numerical libraries. This approach was found to be sufficiently fast for our purposes: Calculating the LDOS for 100 energies at one site of a 200×200 lattice requires ~ 2 min computation time on a modern desktop computer.

Appendix B: Derivation of the RKKY interaction

We here provide a detailed derivation of the RKKY interaction energy E_{RKKY} based on Green function methods. At a high level, our approach is similar to previous derivations by e.g. Schwabe et al. [31]. However, in contrast to Ref. [31], our derivation uses the Keldysh formalism [44] and includes more intermediate steps to make the derivation more accessible.

Our starting point is the following argument. Consider a uniform superconductor described by an unperturbed Green function \check{G}_0 . We now place a classical spin \mathbf{S}_1 at a position \mathbf{R}_1 , which couples to the electrons in the metal via an exchange interaction $\mathcal{H}_{\text{int}} = -(\mathcal{J}/2)\mathbf{S}_1 \cdot \mathbf{s}(\mathbf{R}_1)$, where $\mathbf{s}(\mathbf{r})$ is the electron spin operator at a position \mathbf{r} . This perturbs the Green function from \check{G}_0 to $\check{G} \equiv \check{G}_0 + \delta\check{G}$. This $\delta\check{G}$ then shifts the electron spin density by an amount $\delta\mathbf{s}_1(\mathbf{r})$, which typically oscillates and decays as a function of the distance $|\mathbf{r} - \mathbf{R}_1|$ from the spin \mathbf{S}_1 . If we then place a second spin \mathbf{S}_2 at $\mathbf{r} = \mathbf{R}_2$, this spin interacts with the electron spin density $\delta\mathbf{s}_1(\mathbf{R}_2)$ at that position via a second exchange interaction $-(\mathcal{J}/2)\mathbf{S}_2 \cdot \delta\mathbf{s}_1(\mathbf{R}_2)$. Assuming that $\delta\mathbf{s}_1$ has been calculated to leading order $\mathcal{O}(\mathcal{J})$, the result is an $\mathcal{O}(\mathcal{J}^2)$ contribution to E_{RKKY} . When we also include the inverse process, i.e. how the perturbation $\delta\mathbf{s}_2$ generated by \mathbf{S}_2 affects \mathbf{S}_1 , the RKKY interaction energy can be written:

$$E_{\text{RKKY}} = E_{\text{RKKY}}^{21} + E_{\text{RKKY}}^{12} \\ = (-\mathcal{J}/2)[\mathbf{S}_1 \cdot \delta\mathbf{s}_2(\mathbf{R}_1) + \mathbf{S}_2 \cdot \delta\mathbf{s}_1(\mathbf{R}_2)]. \quad (\text{B1})$$

Below, we only calculate $E_{\text{RKKY}}^{12} \sim \mathbf{S}_2 \cdot \delta\mathbf{s}_1(\mathbf{R}_2)$ explicitly, as the remaining term E_{RKKY}^{21} follows from symmetry.

Note that some terms of similar order have been discarded in the argument above, as we are only interested in deriving the interactions between \mathbf{S}_1 and \mathbf{S}_2 . First, in ferromagnets and non-unitary superconductors, even the unperturbed Green function \check{G}_0 gives rise to a finite spin expectation value $\mathbf{s}(\mathbf{r})$. This yields a lower-order contribution $(-\mathcal{J}/2)[\mathbf{S}_1 \cdot \mathbf{s}(\mathbf{R}_1) + \mathbf{S}_2 \cdot \mathbf{s}(\mathbf{R}_2)]$ to the energy of the system, which is important for understanding the ground-state spin configuration. Second, even in non-magnetic metals, there are two more contributions of the same order as we consider: $(-\mathcal{J}/2)[\mathbf{S}_1 \cdot \delta\mathbf{s}_1(\mathbf{R}_1) + \mathbf{S}_2 \cdot \delta\mathbf{s}_2(\mathbf{R}_2)]$. These terms can be understood as a paramagnetic interaction between the metal and each individual spin. However, none of these contributions correspond to interactions between the two spins \mathbf{S}_1 and \mathbf{S}_2 , and are not considered RKKY interactions.

1. Green function formalism

As mentioned above, we here employ the Keldysh Green function formalism [44]—just generalized from Keldysh \otimes Spin space to Keldysh \otimes Nambu \otimes Spin space, as required to describe superconductors. We thus define the 8×8 matrices

$$\check{G} = \begin{pmatrix} \hat{G}^R & \hat{G}^K \\ & \hat{G}^A \end{pmatrix}, \quad \check{G}_0 = \begin{pmatrix} \hat{G}_0^R & \hat{G}_0^K \\ & \hat{G}_0^A \end{pmatrix}, \quad \check{\Sigma} = \begin{pmatrix} \hat{\Sigma}^R & \hat{\Sigma}^K \\ & \hat{\Sigma}^A \end{pmatrix}, \quad (\text{B2})$$

where quantities with hats are 4×4 matrices in Nambu \otimes Spin space. We now expand the Dyson equation for \check{G} to first order

in the self-energy $\check{\Sigma}$ [44], which yields the following shift $\delta\check{G} = \check{G} - \check{G}_0$ from the unperturbed Green function \check{G}_0 :

$$\delta\check{G} = \check{G}_0 \otimes \check{\Sigma} \otimes \check{G}_0. \quad (\text{B3})$$

Next, consider a classical spin \mathbf{S}_1 placed at \mathbf{R}_1 on the superconductor. This can be modeled using the block-diagonal self-energy matrix $\check{\Sigma} = \text{diag}(\hat{\Sigma}, \hat{\Sigma})$, where the 4×4 self-energy matrix

$$\hat{\Sigma}(1, 2) = -(\beta/2)(\mathbf{S}_1 \cdot \hat{\boldsymbol{\sigma}}) \delta(\mathbf{r}_1 - \mathbf{R}_1) \delta(1 - 2). \quad (\text{B4})$$

We here use the common short-hand notation $1 \rightarrow (\mathbf{r}_1, t_1)$ and $2 \rightarrow (\mathbf{r}_2, t_2)$ for space-time coordinates [44]. Moreover, we have introduced a vector of 4×4 matrices $\hat{\boldsymbol{\sigma}} = \text{diag}(\boldsymbol{\sigma}, \boldsymbol{\sigma}^*)$ [45], where $\boldsymbol{\sigma}$ is the Pauli vector. It can be shown that this self-energy matrix $\check{\Sigma}$ correctly reproduces the Gorkov equation for a metal with a spin impurity [46, 47]. The definition of “ \otimes ” [44] now yields the more explicit equation

$$\delta\check{G}(1, 2) = \int d1' \int d2' \check{G}_0(1, 1') \hat{\Sigma}(1', 2') \check{G}_0(2', 2), \quad (\text{B5})$$

where $d1' \equiv d\mathbf{r}_{1'} dt_{1'}$ and so on. For our purposes, we do not need to determine the whole 8×8 matrix $\delta\check{G}$; it is sufficient to calculate the top-right 4×4 block $\delta\hat{G}^K(1, 2)$. From direct multiplication of the definitions of these matrices, we find

$$\begin{aligned} \delta\hat{G}^K(1, 2) = \int d1' \int d2' \left\{ \hat{G}_0^R(1, 1') \hat{\Sigma}(1', 2') \hat{G}_0^K(2', 2) \right. \\ \left. + \hat{G}_0^K(1, 1') \hat{\Sigma}(1', 2') \hat{G}_0^A(2', 2) \right\}, \end{aligned} \quad (\text{B6})$$

where $\hat{\Sigma}$ is given by Eq. (B4). Since $\hat{\Sigma}(1', 2') \sim \delta(1' - 2')$, the integral over $2'$ is trivial. Moreover, we only require the equal-coordinate Green function $\delta\hat{G}^K(1) \equiv \lim_{2 \rightarrow 1} \delta\hat{G}^K(1, 2)$ to determine the spin density δs_1 that arises. This is because the Green function $\hat{G}^K(1, 2)$ is formally defined in terms of expectation values on the form $\langle \psi_{\sigma_1}^\dagger(\mathbf{r}_1, t_1) \psi_{\sigma_2}(\mathbf{r}_2, t_2) \rangle$, which only correspond to spin-resolved electron number operators when $(\mathbf{r}_1, t_1, \sigma_1)$ and $(\mathbf{r}_2, t_2, \sigma_2)$ are equal. After some relabeling of the remaining coordinates, we thus obtain the equation

$$\begin{aligned} \delta\hat{G}^K(1) = -\frac{\beta}{2} \lim_{3 \rightarrow 1} \int dt_2 \int d\mathbf{r}_2 \delta(\mathbf{r}_2 - \mathbf{R}_1) \\ \times \left\{ \hat{G}_0^R(1, 2) (\mathbf{S}_1 \cdot \hat{\boldsymbol{\sigma}}) \hat{G}_0^K(2, 3) \right. \\ \left. + \hat{G}_0^K(1, 2) (\mathbf{S}_1 \cdot \hat{\boldsymbol{\sigma}}) \hat{G}_0^A(2, 3) \right\}. \end{aligned} \quad (\text{B7})$$

2. Wigner transformation

The next step is to perform a *Wigner transformation* [48]. To keep the notation simple, let us consider the following equation for now, which captures the overall mathematical structure of the actual equation for $\delta\hat{G}^K$ presented in Eq. (B7):

$$\begin{aligned} A(\mathbf{r}_1, t_1) = \lim_{3 \rightarrow 1} \int dt_2 \int d\mathbf{r}_2 \delta(\mathbf{r}_2 - \mathbf{R}_1) \\ \times B(\mathbf{r}_1, t_1 | \mathbf{r}_2, t_2) (\mathbf{S}_1 \cdot \hat{\boldsymbol{\sigma}}) C(\mathbf{r}_2, t_2 | \mathbf{r}_3, t_3). \end{aligned} \quad (\text{B8})$$

We now introduce the following center-of-mass coordinates $(\mathbf{r}_{ij}, t_{ij})$ and relative coordinates $(\boldsymbol{\rho}_{ij}, \tau_{ij})$:

$$\begin{aligned} \mathbf{r}_{ij} &\equiv (\mathbf{r}_i + \mathbf{r}_j)/2, & \boldsymbol{\rho}_{ij} &\equiv \mathbf{r}_i - \mathbf{r}_j, \\ t_{ij} &\equiv (t_i + t_j)/2, & \tau_{ij} &\equiv t_i - t_j. \end{aligned} \quad (\text{B9})$$

In terms of these so-called *mixed coordinates*, we now have

$$\begin{aligned} A(\mathbf{r}_1, t_1) = \lim_{3 \rightarrow 1} \int dt_2 \int d\mathbf{r}_2 \delta(\mathbf{r}_2 - \mathbf{R}_1) \\ \times B(\mathbf{r}_{12}, \boldsymbol{\rho}_{12}, t_{12}, \tau_{12}) (\mathbf{S}_1 \cdot \hat{\boldsymbol{\sigma}}) C(\mathbf{r}_{23}, \boldsymbol{\rho}_{23}, t_{23}, \tau_{23}). \end{aligned} \quad (\text{B10})$$

Next, we Fourier transform relative coordinates $(\boldsymbol{\rho}_{ij}, \tau_{ij})$ into corresponding momentum and energy variables $(\mathbf{p}_{ij}, \omega_{ij})$,

$$\begin{aligned} A(\mathbf{r}_1, t_1) = \lim_{3 \rightarrow 1} \int dt_2 \int d\mathbf{r}_2 \delta(\mathbf{r}_2 - \mathbf{R}_1) \\ \times \int d\omega_{12} e^{i\omega_{12}\tau_{12}} \int d\omega_{23} e^{i\omega_{23}\tau_{23}} \\ \times \int d\mathbf{p}_{12} e^{-i\mathbf{p}_{12} \cdot \boldsymbol{\rho}_{12}} \int d\mathbf{p}_{23} e^{-i\mathbf{p}_{23} \cdot \boldsymbol{\rho}_{23}} \\ \times B(\mathbf{r}_{12}, \mathbf{p}_{12}, t_{12}, \omega_{12}) (\mathbf{S}_1 \cdot \hat{\boldsymbol{\sigma}}) C(\mathbf{r}_{23}, \mathbf{p}_{23}, t_{23}, \omega_{23}). \end{aligned} \quad (\text{B11})$$

Let us now take the limit $\lim_{3 \rightarrow 1} = \lim_{\mathbf{r}_3 \rightarrow \mathbf{r}_1} \lim_{t_3 \rightarrow t_1}$. The implications for the relative variables are that

$$\begin{aligned} \tau_{23} &\equiv t_2 - t_3 \rightarrow t_2 - t_1 \equiv -\tau_{12}, \\ \boldsymbol{\rho}_{23} &\equiv \mathbf{r}_2 - \mathbf{r}_3 \rightarrow \mathbf{r}_2 - \mathbf{r}_1 \equiv -\boldsymbol{\rho}_{12}. \end{aligned} \quad (\text{B12})$$

Moreover, the actual functions B and C we will consider later correspond to components of the *unperturbed* Green function \check{G}_0 of the system—which in our case is assumed to be homogeneous and time independent. This means that B and C are in practice not functions of $\mathbf{r}_{12}, \mathbf{r}_{23}, t_{12}, t_{23}$. With these considerations in mind, the result above simplifies to

$$\begin{aligned} A(\mathbf{r}_1, t_1) = \int dt_2 \int d\mathbf{r}_2 \delta(\mathbf{r}_2 - \mathbf{R}_1) \\ \times \int d\omega_{12} \int d\omega_{23} e^{i\tau_{12}(\omega_{12} - \omega_{23})} \\ \times \int d\mathbf{p}_{12} \int d\mathbf{p}_{23} e^{-i\boldsymbol{\rho}_{12} \cdot (\mathbf{p}_{12} - \mathbf{p}_{23})} \\ \times B(\mathbf{p}_{12}, \omega_{12}) (\mathbf{S}_1 \cdot \hat{\boldsymbol{\sigma}}) C(\mathbf{p}_{23}, \omega_{23}). \end{aligned} \quad (\text{B13})$$

Next, we consider the integrals over t_2 and \mathbf{r}_2 . Since t_1 and \mathbf{r}_1 are held constant during the integration on the right-hand side of the equation, we can write $dt_2 = d(t_2 - t_1) \equiv -d\tau_{12}$ and

$d\mathbf{r}_2 = d(\mathbf{r}_2 - \mathbf{r}_1) \equiv -d\mathbf{p}_{12}$. Thus, we can rewrite the above as

$$A(\mathbf{r}_1, t_1) = \int d\tau_{12} \int d\mathbf{p}_{12} \delta(-\mathbf{p}_{12} + \mathbf{r}_1 - \mathbf{R}_1) \times \int d\omega_{12} \int d\omega_{23} e^{i\tau_{12}(\omega_{12} - \omega_{23})} \times \int d\mathbf{p}_{12} \int d\mathbf{p}_{23} e^{-i\mathbf{p}_{12} \cdot (\mathbf{p}_{12} - \mathbf{p}_{23})} \times B(\mathbf{p}_{12}, \omega_{12}) (S_1 \cdot \hat{\sigma}) C(\mathbf{p}_{23}, \omega_{23}). \quad (\text{B14})$$

Note that the integrand only depends on τ_{12} via the complex exponential. Using the Fourier identity for the delta function,

$$\int d\tau_{12} e^{i\tau_{12}(\omega_{12} - \omega_{23})} = 2\pi \delta(\omega_{12} - \omega_{23}), \quad (\text{B15})$$

and subsequently integrating out ω_{23} , we get

$$A(\mathbf{r}_1, t_1) = 2\pi \int d\mathbf{p}_{12} \delta(-\mathbf{p}_{12} + \mathbf{r}_1 - \mathbf{R}_1) \times \int d\omega_{12} \int d\mathbf{p}_{12} \int d\mathbf{p}_{23} e^{-i\mathbf{p}_{12} \cdot (\mathbf{p}_{12} - \mathbf{p}_{23})} \times B(\mathbf{p}_{12}, \omega_{12}) (S_1 \cdot \hat{\sigma}) C(\mathbf{p}_{23}, \omega_{12}). \quad (\text{B16})$$

Next, we integrate out the spatial variable \mathbf{p}_{12} . The remaining delta function ensures that $\mathbf{p}_{12} \rightarrow \mathbf{r}_1 - \mathbf{R}_1$, so we obtain

$$A(\mathbf{r}_1, t_1) = 2\pi \int d\omega_{12} \int d\mathbf{p}_{12} \int d\mathbf{p}_{23} e^{-i(\mathbf{r}_1 - \mathbf{R}_1) \cdot (\mathbf{p}_{12} - \mathbf{p}_{23})} \times B(\mathbf{p}_{12}, \omega_{12}) (S_1 \cdot \hat{\sigma}) C(\mathbf{p}_{23}, \omega_{12}). \quad (\text{B17})$$

For simplicity, we at this point rename the integration variables $\omega_{12} \rightarrow \omega$, $\mathbf{p}_{12} \rightarrow \mathbf{p}_1$, $\mathbf{p}_{23} \rightarrow \mathbf{p}_2$. As there is no dependence on the absolute time t_1 , this can also be omitted on the left-hand side. The final form of the Wigner transformation is thus

$$A(\mathbf{r}_1) = 2\pi \int d\omega \int d\mathbf{p}_1 \int d\mathbf{p}_2 e^{i(\mathbf{p}_2 - \mathbf{p}_1) \cdot (\mathbf{r}_1 - \mathbf{R}_1)} \times B(\mathbf{p}_1, \omega) (S_1 \cdot \hat{\sigma}) C(\mathbf{p}_2, \omega). \quad (\text{B18})$$

We now apply this transformation to the Green function shift that we obtained in Eq. (B7), which yields the result

$$\delta \hat{G}^K(\mathbf{r}_1) = -\mathcal{J} \pi \int d\omega \int d\mathbf{p}_1 \int d\mathbf{p}_2 e^{i(\mathbf{p}_2 - \mathbf{p}_1) \cdot (\mathbf{r}_1 - \mathbf{R}_1)} \times \left\{ \hat{G}_0^R(\mathbf{p}_1, \omega) (S_1 \cdot \hat{\sigma}) \hat{G}_0^K(\mathbf{p}_2, \omega) + \hat{G}_0^K(\mathbf{p}_1, \omega) (S_1 \cdot \hat{\sigma}) \hat{G}_0^A(\mathbf{p}_2, \omega) \right\}. \quad (\text{B19})$$

3. Spin expectation value

Once the equal-coordinate Keldysh Green function $\hat{G}^K(\mathbf{r})$ is known, the electron spin density follows directly from [49]

$$\mathbf{s}(\mathbf{r}) = \frac{1}{8} \text{Im Tr}[\hat{\sigma} \hat{G}^K(\mathbf{r})]. \quad (\text{B20})$$

Thus, in the kind of system treated in the previous subsections, we find the following perturbation of the spin density

$$\delta s_1(\mathbf{r}) = \frac{1}{8} \text{Im Tr}[\hat{\sigma} \delta \hat{G}^K(\mathbf{r})]. \quad (\text{B21})$$

The contribution to Eq. (B1) then becomes

$$E_{\text{RKKY}}^{12} = -\frac{\mathcal{J}}{2} S_2 \cdot \delta s_1(\mathbf{R}_2) = -\frac{\mathcal{J}}{16} \text{Im Tr}[(S_2 \cdot \hat{\sigma}) \delta \hat{G}^K(\mathbf{R}_2)]. \quad (\text{B22})$$

We can now substitute Eq. (B19) into this result, and find

$$E_{\text{RKKY}}^{12} = \frac{\pi \mathcal{J}^2}{16} \text{Im} \int d\omega \int d\mathbf{p}_1 \int d\mathbf{p}_2 e^{i(\mathbf{p}_2 - \mathbf{p}_1) \cdot (\mathbf{R}_2 - \mathbf{R}_1)} \times \text{Tr} \left\{ (S_2 \cdot \hat{\sigma}) \hat{G}_0^R(\mathbf{p}_1, \omega) (S_1 \cdot \hat{\sigma}) \hat{G}_0^K(\mathbf{p}_2, \omega) + (S_2 \cdot \hat{\sigma}) \hat{G}_0^K(\mathbf{p}_1, \omega) (S_1 \cdot \hat{\sigma}) \hat{G}_0^A(\mathbf{p}_2, \omega) \right\}. \quad (\text{B23})$$

Note that this is a quite general result: We have performed a leading-order perturbation expansion in \mathcal{J} , but have not made any assumptions about the unperturbed system described by \hat{G}_0 except for homogeneity in space and time. Thus, the same equation can be used to describe e.g. superconductors, magnets, or spin-orbit-coupled systems. Moreover, the result obtained at this point is valid both in and out of equilibrium.

4. Thermodynamic equilibrium

The Keldysh Green function can be parametrized in terms of a 4×4 distribution function matrix \hat{h} [44, 50],

$$\hat{G}_0^K = \hat{G}_0^R \hat{h} - \hat{h} \hat{G}_0^A. \quad (\text{B24})$$

In equilibrium, electrons follow the Fermi-Dirac distribution, which is described by $\hat{h} = \tanh(\omega/2T) \hat{\tau}_0$, where T is the temperature and $\hat{\tau}_0$ is an identity matrix. Thus, we find that

$$\hat{G}_0^K = (\hat{G}_0^R - \hat{G}_0^A) \tanh(\omega/2T). \quad (\text{B25})$$

Another useful symmetry which follows from the definitions of the Green functions [47], is that $\hat{G}^A = (\hat{\tau}_3 \hat{G}^R \hat{\tau}_3)^\dagger$, where $\hat{\tau}_3 = \text{diag}(+1, +1, -1, -1)$ is a Pauli matrix in Nambu space. This lets us further simplify the relation above to

$$\hat{G}_0^K = (\hat{G}_0^R - \hat{\tau}_3 \hat{G}_0^{R\dagger} \hat{\tau}_3) \tanh(\omega/2T). \quad (\text{B26})$$

Using the short-hand notation $\hat{G}_i^R = \hat{G}_0^R(\mathbf{p}_i, \omega)$ for brevity, the above lets us rewrite our equation for the RKKY interaction as

$$\begin{aligned}
E_{\text{RKKY}}^{12} = & \frac{\pi\mathcal{J}^2}{16} \text{Im} \int d\omega \tanh(\omega/2T) \\
& \times \int d\mathbf{p}_1 \int d\mathbf{p}_2 e^{i(\mathbf{p}_2 - \mathbf{p}_1) \cdot (\mathbf{R}_2 - \mathbf{R}_1)} \\
& \times \text{Tr} \left\{ (S_2 \cdot \hat{\sigma}) \hat{G}_1^R (S_1 \cdot \hat{\sigma}) \hat{G}_2^R \right. \\
& - (S_2 \cdot \hat{\sigma}) \hat{G}_1^R (S_1 \cdot \hat{\sigma}) \hat{\tau}_3 \hat{G}_2^{R\dagger} \hat{\tau}_3 \\
& + (S_2 \cdot \hat{\sigma}) \hat{G}_1^R (S_1 \cdot \hat{\sigma}) \hat{\tau}_3 \hat{G}_2^{R\dagger} \hat{\tau}_3 \\
& \left. - (S_2 \cdot \hat{\sigma}) \hat{\tau}_3 \hat{G}_1^{R\dagger} \hat{\tau}_3 (S_1 \cdot \hat{\sigma}) \hat{\tau}_3 \hat{G}_2^{R\dagger} \hat{\tau}_3 \right\}. \tag{B27}
\end{aligned}$$

Clearly, the second and third terms in the trace cancel. The remaining terms can be simplified using the fact that $[\hat{\tau}_3, \hat{\sigma}] = 0$ together with the cyclic trace rule:

$$\begin{aligned}
E_{\text{RKKY}}^{12} = & \frac{\pi\mathcal{J}^2}{16} \text{Im} \int d\omega \tanh(\omega/2T) \\
& \times \int d\mathbf{p}_1 \int d\mathbf{p}_2 e^{i(\mathbf{p}_2 - \mathbf{p}_1) \cdot (\mathbf{R}_2 - \mathbf{R}_1)} \\
& \times \text{Tr} \left\{ (S_2 \cdot \hat{\sigma}) \hat{G}_1^R (S_1 \cdot \hat{\sigma}) \hat{G}_2^R \right. \\
& \left. - (S_2 \cdot \hat{\sigma}) \hat{G}_1^{R\dagger} (S_1 \cdot \hat{\sigma}) \hat{G}_2^{R\dagger} \right\}. \tag{B28}
\end{aligned}$$

To further simplify this result, we observe that:

$$\begin{aligned}
& \left\{ \int d\mathbf{p}_1 \int d\mathbf{p}_2 e^{i(\mathbf{p}_2 - \mathbf{p}_1) \cdot (\mathbf{R}_2 - \mathbf{R}_1)} \text{Tr} \left[(S_2 \cdot \hat{\sigma}) \hat{G}_1^R (S_1 \cdot \hat{\sigma}) \hat{G}_2^R \right] \right\}^* \\
& = \int d\mathbf{p}_1 \int d\mathbf{p}_2 e^{-i(\mathbf{p}_2 - \mathbf{p}_1) \cdot (\mathbf{R}_2 - \mathbf{R}_1)} \text{Tr} \left[(S_2 \cdot \hat{\sigma}) \hat{G}_1^R (S_1 \cdot \hat{\sigma}) \hat{G}_2^R \right]^\dagger \\
& = \int d\mathbf{p}_1 \int d\mathbf{p}_2 e^{i(\mathbf{p}_1 - \mathbf{p}_2) \cdot (\mathbf{R}_2 - \mathbf{R}_1)} \text{Tr} \left[\hat{G}_2^{R\dagger} (S_1 \cdot \hat{\sigma}) \hat{G}_1^{R\dagger} (S_2 \cdot \hat{\sigma}) \right] \\
& = \int d\mathbf{p}_1 \int d\mathbf{p}_2 e^{i(\mathbf{p}_1 - \mathbf{p}_2) \cdot (\mathbf{R}_2 - \mathbf{R}_1)} \text{Tr} \left[(S_2 \cdot \hat{\sigma}) \hat{G}_2^{R\dagger} (S_1 \cdot \hat{\sigma}) \hat{G}_1^{R\dagger} \right] \\
& = \int d\mathbf{p}_2 \int d\mathbf{p}_1 e^{i(\mathbf{p}_2 - \mathbf{p}_1) \cdot (\mathbf{R}_2 - \mathbf{R}_1)} \text{Tr} \left[(S_2 \cdot \hat{\sigma}) \hat{G}_1^{R\dagger} (S_1 \cdot \hat{\sigma}) \hat{G}_2^{R\dagger} \right]
\end{aligned}$$

where in the last step we relabeled the momentum variables $\mathbf{p}_1 \leftrightarrow \mathbf{p}_2$ (which by definition also implies $\hat{G}_1^R \leftrightarrow \hat{G}_2^R$). We now substitute this result into Eq. (B28), use the general identity $z - z^* = 2i \text{Im} z$, and reinstate the definitions of \hat{G}_i^R :

$$\begin{aligned}
E_{\text{RKKY}}^{12} = & \frac{\pi\mathcal{J}^2}{8} \text{Im} \int d\omega \tanh(\omega/2T) \\
& \times \int d\mathbf{p}_1 \int d\mathbf{p}_2 e^{i(\mathbf{p}_2 - \mathbf{p}_1) \cdot (\mathbf{R}_2 - \mathbf{R}_1)} \\
& \times \text{Tr} \left\{ (S_2 \cdot \hat{\sigma}) \hat{G}_0^R(\mathbf{p}_1, \omega) (S_1 \cdot \hat{\sigma}) \hat{G}_0^R(\mathbf{p}_2, \omega) \right\}, \tag{B29}
\end{aligned}$$

The other contribution E_{RKKY}^{21} can be obtained by letting $S_1 \leftrightarrow S_2$ and $\mathbf{R}_1 \leftrightarrow \mathbf{R}_2$. Using the cyclic trace rule, and again relabeling momentum variables $\mathbf{p}_1 \leftrightarrow \mathbf{p}_2$, one can then show that $E_{\text{RKKY}}^{12} = E_{\text{RKKY}}^{21}$. Thus, we can write the final equation for the interaction energy $E_{\text{RKKY}} = E_{\text{RKKY}}^{12} + E_{\text{RKKY}}^{21}$ as

$$\begin{aligned}
E_{\text{RKKY}} = & \frac{\pi\mathcal{J}^2}{4} \text{Im} \int d\omega \tanh(\omega/2T) \\
& \times \int d\mathbf{p}_1 \int d\mathbf{p}_2 e^{-i(\mathbf{p}_2 - \mathbf{p}_1) \cdot (\mathbf{R}_2 - \mathbf{R}_1)} \\
& \times \text{Tr} \left\{ (S_1 \cdot \hat{\sigma}) \hat{G}_0^R(\mathbf{p}_1, \omega) (S_2 \cdot \hat{\sigma}) \hat{G}_0^R(\mathbf{p}_2, \omega) \right\}. \tag{B30}
\end{aligned}$$

This result is valid for general translation-invariant superconductors in equilibrium, and can be evaluated as long as its unperturbed Green function $\hat{G}_0^R(\mathbf{p}, \omega)$ is known.

Appendix C: RKKY interactions in superconductors

In Appendix B, we derived Eq. (B30) for the RKKY interaction energy E_{RKKY} in a translation-invariant superconductor described by a Green function $\hat{G}_0^R(\mathbf{p}, \omega)$. We now specialize to the case where \hat{G}_0^R describes a p -wave triplet superconductor, and explore how E_{RKKY} depends on the symmetries of its order parameter. First, let us rewrite Eq. (B30) as

$$\begin{aligned}
E_{\text{RKKY}} = & \frac{\pi}{4} \mathcal{J}^2 \text{Im} \int d\mathbf{p}_1 \int d\mathbf{p}_2 e^{-i(\mathbf{p}_2 - \mathbf{p}_1) \cdot (\mathbf{R}_2 - \mathbf{R}_1)} \\
& \times \int d\omega \tanh(\omega/2T) \mathcal{T}(S_1, S_2, \mathbf{p}_1, \mathbf{p}_2, \omega), \tag{C1}
\end{aligned}$$

where the function \mathcal{T} at the end refers to the trace

$$\mathcal{T} = \text{Tr} \left[(S_1 \cdot \hat{\sigma}) \hat{G}_1 (S_2 \cdot \hat{\sigma}) \hat{G}_2 \right], \tag{C2}$$

and we for brevity use the short-hand notation $\hat{G}_i \equiv \hat{G}_0^R(\mathbf{p}_i, \omega)$ for the relevant Green function from here on. The structure of the matrices \hat{G}_i and $\hat{\sigma}_i$ in Nambu space is

$$\hat{G}_i = \begin{pmatrix} G_i & F_i \\ \tilde{F}_i & \tilde{G}_i \end{pmatrix}, \quad \hat{\sigma} = \begin{pmatrix} \sigma & \\ & \sigma^* \end{pmatrix}, \tag{C3}$$

where $\tilde{X}(\mathbf{p}, \omega) \equiv X^*(-\mathbf{p}, -\omega)$. The 2×2 spin matrices G_i and F_i are referred to as the normal and anomalous Green functions, respectively. The normal Green function describes quasiparticles (electrons and holes), whereas the anomalous Green function describes superconducting correlations (Cooper pairs). If we substitute these matrices into the bracketed expression in Eq. (C2), and perform an explicit matrix multiplication, we see that the diagonal entries which contribute to the trace are

$$(S_1 \cdot \hat{\sigma}) \hat{G}_1 (S_2 \cdot \hat{\sigma}) \hat{G}_2 = \begin{pmatrix} (S_1 \cdot \sigma) G_1 (S_2 \cdot \sigma) G_2 + (S_1 \cdot \sigma) F_1 (S_2 \cdot \sigma^*) \tilde{F}_2 & \dots \\ \dots & (S_1 \cdot \sigma^*) \tilde{G}_1 (S_2 \cdot \sigma^*) \tilde{G}_2 + (S_1 \cdot \sigma^*) \tilde{F}_1 (S_2 \cdot \sigma) F_2 \end{pmatrix}. \quad (C4)$$

Clearly, the bottom-right block is just the “tilde conjugate” of the top-left block. Thus, taking the trace of this result yields

$$\mathcal{T} = \mathcal{G} + \tilde{\mathcal{G}} + \mathcal{F} + \tilde{\mathcal{F}}, \quad (C5)$$

$$\mathcal{G} \equiv \text{Tr}[(S_1 \cdot \sigma) G_1 (S_2 \cdot \sigma) G_2], \quad (C6)$$

$$\mathcal{F} \equiv \text{Tr}[(S_1 \cdot \sigma) F_1 (S_2 \cdot \sigma^*) \tilde{F}_2]. \quad (C7)$$

Here, the RKKY interactions mediated by quasiparticles and superconductivity, respectively, are contained in \mathcal{G} and \mathcal{F} .

Next, let us rewrite the contributions from $\tilde{\mathcal{G}}$ and $\tilde{\mathcal{F}}$ in terms of \mathcal{G} and \mathcal{F} . Let us first combine Eq. (C1) with the definition of tilde conjugation, and then redefine the integration variables $\{\mathbf{p}_1, \mathbf{p}_2, \omega\} \rightarrow \{-\mathbf{p}_1, -\mathbf{p}_2, -\omega\}$. This shows us that:

$$\begin{aligned} & \int d\mathbf{p}_1 d\mathbf{p}_2 d\omega e^{-i(\mathbf{p}_2 - \mathbf{p}_1) \cdot \delta \mathbf{R}} \tanh(\omega/2T) \tilde{\mathcal{X}}(\mathbf{p}_1, \mathbf{p}_2, \omega) \\ & \equiv \int d\mathbf{p}_1 d\mathbf{p}_2 d\omega e^{-i(\mathbf{p}_2 - \mathbf{p}_1) \cdot \delta \mathbf{R}} \tanh(\omega/2T) \mathcal{X}^*(-\mathbf{p}_1, -\mathbf{p}_2, -\omega) \\ & = \int d\mathbf{p}_1 d\mathbf{p}_2 d\omega e^{+i(\mathbf{p}_2 - \mathbf{p}_1) \cdot \delta \mathbf{R}} \tanh(-\omega/2T) \mathcal{X}^*(\mathbf{p}_1, \mathbf{p}_2, \omega) \\ & = - \left\{ \int d\mathbf{p}_1 d\mathbf{p}_2 d\omega e^{-i(\mathbf{p}_2 - \mathbf{p}_1) \cdot \delta \mathbf{R}} \tanh(\omega/2T) \mathcal{X}(\mathbf{p}_1, \mathbf{p}_2, \omega) \right\}^*, \end{aligned}$$

where the bracketed expression is simply the corresponding contribution from \mathcal{X} . Since $z - z^* = 2i \text{Im } z$, we conclude that

$$\begin{aligned} E_{\text{RKKY}} &= \frac{1}{2} \pi \delta^2 \text{Im} \int d\mathbf{p}_1 \int d\mathbf{p}_2 e^{-i(\mathbf{p}_2 - \mathbf{p}_1) \cdot (\mathbf{R}_2 - \mathbf{R}_1)} \\ & \quad \times \int d\omega \tanh(\omega/2T) (\mathcal{G} + \mathcal{F}), \end{aligned} \quad (C8)$$

which shows that we do not need to explicitly calculate the tilde-conjugated contributions $\tilde{\mathcal{G}}$ and $\tilde{\mathcal{F}}$ to evaluate E_{RKKY} .

Although the quasiparticle contributions \mathcal{G} to the RKKY interaction are modulated by the opening of a superconducting gap [9], we will here focus on the contributions \mathcal{F} that arise more directly from superconducting correlations. Moreover, we are particularly interested in triplet superconductors, and will therefore consider the anomalous Green function

$$F_i = (\mathbf{d}_i \cdot \sigma) i\sigma_2, \quad (C9)$$

where $\mathbf{d}_i = \mathbf{d}(\mathbf{p}_i, \omega)$ is closely related to the conventional \mathbf{d} -vector [15]. Note that we here use $\mathbf{d}(\mathbf{p}, \omega)$ to parametrize the Green function $F(\mathbf{p}, \omega)$ as opposed to the order parameter $\Delta(\mathbf{p})$; these are related by a distribution-weighted energy integral. To determine the E_{RKKY} , we now have to evaluate

$$\mathcal{F} = -\text{Tr}[(S_1 \cdot \sigma)(\mathbf{d}_1 \cdot \sigma)\sigma_2(S_2 \cdot \sigma^*)(\tilde{\mathbf{d}}_2 \cdot \sigma^*)\sigma_2]. \quad (C10)$$

We now use $\sigma_0 = (\sigma_2)^2$ to insert an extra pair of σ_2 matrices between $(S_2 \cdot \sigma^*)$ and $(\tilde{\mathbf{d}}_2 \cdot \sigma^*)$, and then use $\sigma_2 \sigma_2 = -\sigma^*$ to get rid of all σ_2 factors. This yields the result

$$\mathcal{F} = -\text{Tr}[(S_1 \cdot \sigma)(\mathbf{d}_1 \cdot \sigma)(S_2 \cdot \sigma)(\tilde{\mathbf{d}}_2 \cdot \sigma)]. \quad (C11)$$

Next, we invoke the Pauli vector identity

$$(\mathbf{a} \cdot \sigma)(\mathbf{b} \cdot \sigma) = (\mathbf{a} \cdot \mathbf{b})\sigma_0 + i(\mathbf{a} \times \mathbf{b}) \cdot \sigma \quad (C12)$$

twice in order to write the trace above as

$$\mathcal{F} = -\text{Tr}\{[(S_1 \cdot \mathbf{d}_1)\sigma_0 + i(S_1 \times \mathbf{d}_1) \cdot \sigma][(S_2 \cdot \tilde{\mathbf{d}}_2)\sigma_0 + i(S_2 \times \tilde{\mathbf{d}}_2) \cdot \sigma]\}. \quad (C13)$$

Since $\text{Tr } \sigma_0$ is finite but $\text{Tr } \sigma$ is not, only terms of order $\mathcal{O}(\sigma^0)$ or $\mathcal{O}(\sigma^2)$ survive in the trace above. Thus, we get

$$\mathcal{F} = -\text{Tr}\{[(S_1 \cdot \mathbf{d}_1)(S_2 \cdot \tilde{\mathbf{d}}_2)\sigma_0] - [(S_1 \times \mathbf{d}_1) \cdot \sigma][(S_2 \times \tilde{\mathbf{d}}_2) \cdot \sigma]\}. \quad (C14)$$

We can now again use the Pauli vector identity above in the second term, and the terms that survive the trace are now

$$\mathcal{F} = -\text{Tr}\{[(S_1 \cdot \mathbf{d}_1)(S_2 \cdot \tilde{\mathbf{d}}_2)\sigma_0] - [(S_1 \times \mathbf{d}_1) \cdot (S_2 \times \tilde{\mathbf{d}}_2)\sigma_0]\}. \quad (C15)$$

Taking the trace of this result, we find that

$$\mathcal{F} = -2(S_1 \cdot \mathbf{d}_1)(S_2 \cdot \tilde{\mathbf{d}}_2) + 2(S_1 \times \mathbf{d}_1) \cdot (S_2 \times \tilde{\mathbf{d}}_2). \quad (C16)$$

We can simplify the last term above via the quadruple product identity $(\mathbf{a} \times \mathbf{b}) \cdot (\mathbf{c} \times \mathbf{d}) = (\mathbf{a} \cdot \mathbf{c})(\mathbf{b} \cdot \mathbf{d}) - (\mathbf{a} \cdot \mathbf{d})(\mathbf{b} \cdot \mathbf{c})$,

$$\begin{aligned} \mathcal{F} &= -2(S_1 \cdot \mathbf{d}_1)(S_2 \cdot \tilde{\mathbf{d}}_2) \\ & \quad + 2(\mathbf{d}_1 \cdot \tilde{\mathbf{d}}_2)(S_1 \cdot S_2) \\ & \quad - 2(S_1 \cdot \tilde{\mathbf{d}}_2)(S_2 \cdot \mathbf{d}_1). \end{aligned} \quad (C17)$$

Note that the quadruple product identity above also implies

$$(\mathbf{d}_1 \times \tilde{\mathbf{d}}_2) \cdot (S_1 \times S_2) = (\mathbf{d}_1 \cdot S_1)(\tilde{\mathbf{d}}_2 \cdot S_2) - (\mathbf{d}_1 \cdot S_2)(\tilde{\mathbf{d}}_2 \cdot S_1), \quad (C18)$$

which can be reordered as

$$(S_1 \cdot \tilde{\mathbf{d}}_2)(S_2 \cdot \mathbf{d}_1) = (S_1 \cdot \mathbf{d}_1)(S_2 \cdot \tilde{\mathbf{d}}_2) - (\mathbf{d}_1 \times \tilde{\mathbf{d}}_2) \cdot (S_1 \times S_2). \quad (C19)$$

Finally, we substitute this back into Eq. (C17), and obtain:

$$\begin{aligned} \mathcal{F} &= -4(S_1 \cdot \mathbf{d}_1)(S_2 \cdot \tilde{\mathbf{d}}_2) \\ & \quad + 2(\mathbf{d}_1 \cdot \tilde{\mathbf{d}}_2)(S_1 \cdot S_2) \\ & \quad + 2(\mathbf{d}_1 \times \tilde{\mathbf{d}}_2) \cdot (S_1 \times S_2). \end{aligned} \quad (C20)$$

This is our result for the direct contribution to E_{RKKY} [Eq. (C8)] from p -wave triplet superconductivity.

- [1] M. A. Ruderman and C. Kittel, *Physical Review* **96**, 99 (1954).
- [2] T. Kasuya, *Progress of Theoretical Physics* **16**, 45 (1956).
- [3] K. Yosida, *Physical Review* **106**, 893 (1957).
- [4] Y. Yafet, *Phys. Rev. B* **36**, 3948 (1987).
- [5] H. Imamura, P. Bruno, and Y. Utsumi, *Physical Review B* **69**, 121303 (2004).
- [6] N. E. Alekseevskii, I. A. Garifullin, B. I. Kochelaev, and E. G. Kharakhash'yan, *Zh. Eksp. Teor. Fiz.* **72**, 1523 (1977).
- [7] B. Kochelaev, L. Tagirov, and M. Khusainov, *Zh. Eksp. Teor. Fiz.* **76**, 578 (1979).
- [8] M. Khusainov, *Zh. Eksp. Teor. Fiz.* **109**, 524 (1996).
- [9] D. N. Aristov, S. V. Maleyev, and A. G. Yashenkin, *Zeitschrift für Physik B Condensed Matter* **102**, 467 (1997).
- [10] A. Di Bernardo, S. Komori, G. Livanas, G. Divitini, P. Gentile, M. Cuoco, and J. W. A. Robinson, *Nature Materials* **18**, 1194 (2019).
- [11] M. Shiranzaei, H. Cheraghchi, and F. Parhizgar, *Phys. Rev. B* **96**, 024413 (2017).
- [12] J.-J. Zhu, D.-X. Yao, S.-C. Zhang, and K. Chang, *Phys. Rev. Lett.* **106**, 097201 (2011).
- [13] Q. Liu, C.-X. Liu, C. Xu, X.-L. Qi, and S.-C. Zhang, *Phys. Rev. Lett.* **102**, 156603 (2009).
- [14] J. Bardeen, L. N. Cooper, and J. R. Schrieffer, *Physical Review* **106**, 162 (1957).
- [15] A. P. Mackenzie and Y. Maeno, *Reviews of Modern Physics* **75**, 657 (2003).
- [16] A. Ghanbari and J. Linder, *Physical Review B* **104**, 094527 (2021).
- [17] H. Ding, Y. Hu, M. T. Randeria, S. Hoffman, D. Oindila, J. Klinovaja, D. Loss, and A. Yazdani, *Proc. Natl. Acad. Sci. USA* **118**, e2024837118 (2021).
- [18] A. Villas, R. L. Klees, G. Morrás, H. Huang, C. R. Ast, G. Rastelli, W. Belzig, and J. C. Cuevas, *Phys. Rev. B* **103**, 155407 (2021).
- [19] L. Yu, *Acta Phys. Sin.* **21**, 75 (1965).
- [20] H. Shiba, *Prog. Theor. Phys.* **40**, 435 (1968).
- [21] A. I. Rusinov, *Zh. Eksp. Teor. Fiz.* **56**, 2047 (1969).
- [22] A. Ghanbari, E. Erlandsen, and J. Linder, *Physical Review B* **104**, 054502 (2021).
- [23] S. S. Saxena, P. Agarwal, K. Ahilan, F. M. Grosche, R. K. W. Haselwimer, M. J. Steiner, E. Pugh, I. R. Walker, S. R. Julian, P. Monthoux, G. G. Lonzarich, A. Huxley, I. Sheikin, D. Braithwaite, and J. Flouquet, *Nature* **406**, 587 (2000).
- [24] D. Aoki, A. Huxley, E. Ressouche, D. Braithwaite, J. Flouquet, J.-P. Brison, E. Lhotel, and P. C., *Nature* **413**, 613 (2001).
- [25] J. Alicea, *Rep. Prog. Phys.* **75**, 076501 (2012).
- [26] P. Virtanen, R. Gommers, T. E. Oliphant, M. Haberland, T. Reddy, D. Cournapeau, E. Burovski, P. Peterson, W. Weckesser, J. Bright, S. J. Van Der Walt, M. Brett, J. Wilson, K. J. Millman, N. Mayorov, A. R. J. Nelson, E. Jones, R. Kern, E. Larson, C. J. Carey, Í. Polat, Y. Feng, E. W. Moore, J. VanderPlas, D. Laxalde, J. Perktold, R. Cimrman, I. Henriksen, E. A. Quintero, C. R. Harris, A. M. Archibald, A. H. Ribeiro, F. Pedregosa, P. Van Mulbregt, SciPy 1.0 Contributors, A. Vijaykumar, A. P. Bardelli, A. Rothberg, A. Hilboll, A. Kloeckner, A. Scopatz, A. Lee, A. Rokem, C. N. Woods, C. Fulton, C. Masson, C. Häggström, C. Fitzgerald, D. A. Nicholson, D. R. Hagen, D. V. Pasechnik, E. Olivetti, E. Martin, E. Wieser, F. Silva, F. Lenders, F. Wilhelm, G. Young, G. A. Price, G.-L. Ingold, G. E. Allen, G. R. Lee, H. Audren, I. Probst, J. P. Dietrich, J. Silterra, J. T. Webber, J. Slavič, J. Nothman, J. Buchner, J. Kulick, J. L. Schönberger, J. V. De Miranda Cardoso, J. Reimer, J. Harrington, J. L. C. Rodríguez, J. Nunez-Iglesias, J. Kuczynski, K. Tritz, M. Thoma, M. Newville, M. Kümmerer, M. Bolingbroke, M. Tartre, M. Pak, N. J. Smith, N. Nowaczyk, N. Shebanov, O. Pavlyk, P. A. Brodtkorb, P. Lee, R. T. McGibbon, R. Feldbauer, S. Lewis, S. Tygier, S. Sievert, S. Vigna, S. Peterson, S. More, T. Pudlik, T. Oshima, T. J. Pingel, T. P. Robitaille, T. Spura, T. R. Jones, T. Cera, T. Leslie, T. Zito, T. Krauss, U. Upadhyay, Y. O. Halchenko, and Y. Vázquez-Baeza, *Nature Methods* **17**, 261 (2020).
- [27] Performance-wise, we found the *Intel Distribution for Python* to be most efficient, which ships an optimized version of SciPy that makes use of the *Intel Math Kernel Library*. We also note that there was a significant performance increase by only calculating the eigenvalues (and not the corresponding eigenvectors).
- [28] A. Ghanbari, V. K. Risinggård, and J. Linder, *Scientific Reports* **11**, 5028 (2021).
- [29] A. Yazdani, B. A. Jones, C. P. Lutz, M. F. Crommie, and D. M. Eigler, *Science* **275**, 1767 (1997).
- [30] L. Farinacci, G. Ahmadi, G. Reece, M. Ruby, N. Bogdanoff, O. Peters, B. W. Heinrich, F. Von Oppen, and K. J. Franke, *Physical Review Letters* **121**, 196803 (2018).
- [31] N. F. Schwabe, R. J. Elliott, and N. S. Wingreen, *Physical Review B* **54**, 12953 (1996).
- [32] S.-X. Wang, H.-R. Chang, and J. Zhou, *Physical Review B* **96**, 115204 (2017).
- [33] A. I. Buzdin, *Rev. Mod. Phys.* **77**, 935 (2005).
- [34] F. S. Bergeret, A. F. Volkov, and K. B. Efetov, *Rev. Mod. Phys.* **77**, 1321 (2005).
- [35] J. Linder and J. W. A. Robinson, *Nat. Phys.* **11**, 307 (2015).
- [36] M. Eschrig, *Rep. Prog. Phys.* **78**, 104501 (2015).
- [37] I. Dzyaloshinsky, *Journal of Physics and Chemistry of Solids* **4**, 241 (1958).
- [38] T. Moriya, *Physical Review* **120**, 91 (1960).
- [39] To see this explicitly, we write out the free energy of a system with only Heisenberg and Ising interactions between two spins:
- $$\begin{aligned}\mathcal{F} &= \bar{J} S_1 \cdot S_2 - \delta J S_{1z} S_{2z} \\ &= \bar{J} S_{1x} S_{2x} + \bar{J} S_{1y} S_{2y} + (\bar{J} - \delta J) S_{1z} S_{2z} \\ &= (\bar{J} - \delta J) S_1 \cdot S_2 + \delta J S_{1x} S_{2x} + \delta J S_{1y} S_{2y}.\end{aligned}$$
- Thus, these two are equivalent: (i) Heisenberg interaction \bar{J} and Ising interaction $-\delta J$ along the z axis; (ii) Heisenberg interaction $\bar{J} - \delta J$ and Ising interaction $+\delta J$ along the x and y axes.
- [40] S. Y. Wu, Z. L. Xie, and N. Potoczak, *Physical Review B* **48**, 14826 (1993).
- [41] Y. Nagai, Y. Shinohara, Y. Futamura, and T. Sakurai, *Journal of the Physical Society of Japan* **86**, 014708 (2017).
- [42] L. Covaci, F. M. Peeters, and M. Berciu, *Physical Review Letters* **105**, 167006 (2010).
- [43] A. Weiße, G. Wellein, A. Alvermann, and H. Fehske, *Reviews of Modern Physics* **78**, 275 (2006).
- [44] J. Rammer and H. Smith, *Reviews of Modern Physics* **58**, 323 (1986).
- [45] We define the Green functions such that the Gorkov equation takes the form $[i\hat{\tau}_3\partial_t - \hat{H}]\hat{G}(1, 2) = \delta(1 - 2)$, where $\hat{\tau}_3$ is the third Pauli matrix in Nambu space. Some authors do not include $\hat{\tau}_3$ here, in which case the sign structure of \hat{G} changes. One must then compensate by including an additional sign difference between electrons and holes such that $\hat{\sigma} \rightarrow \text{diag}(+\sigma, -\sigma^*)$.
- [46] L. P. Gorkov, *Soviet Physics JETP* **34**, 505 (1958).
- [47] J. P. Morten, *Spin and Charge Transport in Dirty Superconductors*, MSc thesis, NTNU, Trondheim (2003).

- [48] T. Kita, [Progress of Theoretical Physics](#) **123**, 581 (2010).
- [49] See e.g. the supplemental of Ref. [51] for a complete derivation. Note that we here formulate the equation in terms of the 4×4 matrix \hat{G}^K in Spin \otimes Nambu space, not its top-left 2×2 block G^K .
- [50] W. Belzig, F. K. Wilhelm, C. Bruder, G. Schön, and A. D. Zaikin, [Superlattices and Microstructures](#) **25**, 1251 (1999).
- [51] J. A. Ouassou, J. W. A. Robinson, and J. Linder, [Scientific Reports](#) **9**, 12731 (2019).